Chapter 4 RESULTS AND DISCUSSION

4.1 Optimization of process parameters for Daptomycin production by *Streptomyces roseosporus* using one-factor-at-a-time OFAT method

In order to evaluate the effect of various process parameters and media constituents affecting the growth of the producer strain and the production of Daptomycin, various experiments have been carried out using one-factor-at-a-time method (OFAT) i.e. varying one process parameter at a time and keeping other factors constant in shake flask culture.

4.1.1 Effect of temperature

In order to optimize the temperature for maximum Daptomycin production, *S. roseosporus* was grown in shake flask containing fermentation medium at different temperatures in the range of 20°C-40°C at 200 rpm. All other cultural conditions were kept identical. According to the time course study of the Daptomycin production in the fermentation medium, production was found to be maximum at 144 hours so the samples were taken out at this time to evaluate the Daptomycin concentration [Yu *et al*., 2011]. The data shown in Figure 4.1, revealed that the growth of the cell mass as well as the production of Daptomycin was found to be increased with the rise in temperature up to 30°C, afterwards both cell mass and Daptomycin production decreased with increase in temperature. Therefore, 30°C incubation temperature was found to be optimum for growth and maximum Daptomycin production and was used for further studies.

Temperature affects the activity of enzymes present in the microorganism essential for the antibiotic production. Low temperature leads to decreased enzymatic activity, metabolic regulatory mechanisms and diffusional limitations such as the rate of transport

of nutrients and products in or out of the cells. At higher temperatures, thermal denaturation of protein, enzymes and cellular structures occur. As *S. roseosporus* is soil actinomycetes, its growth is most favored at temperatures between 28-30°C [Huber *et al*., 1987]. Most of Daptomycin production and optimization studies in previous literatures have been done using the temperature range of 28-30°C [Yu *et al*., 2011 and Lu *et al*., 2011].

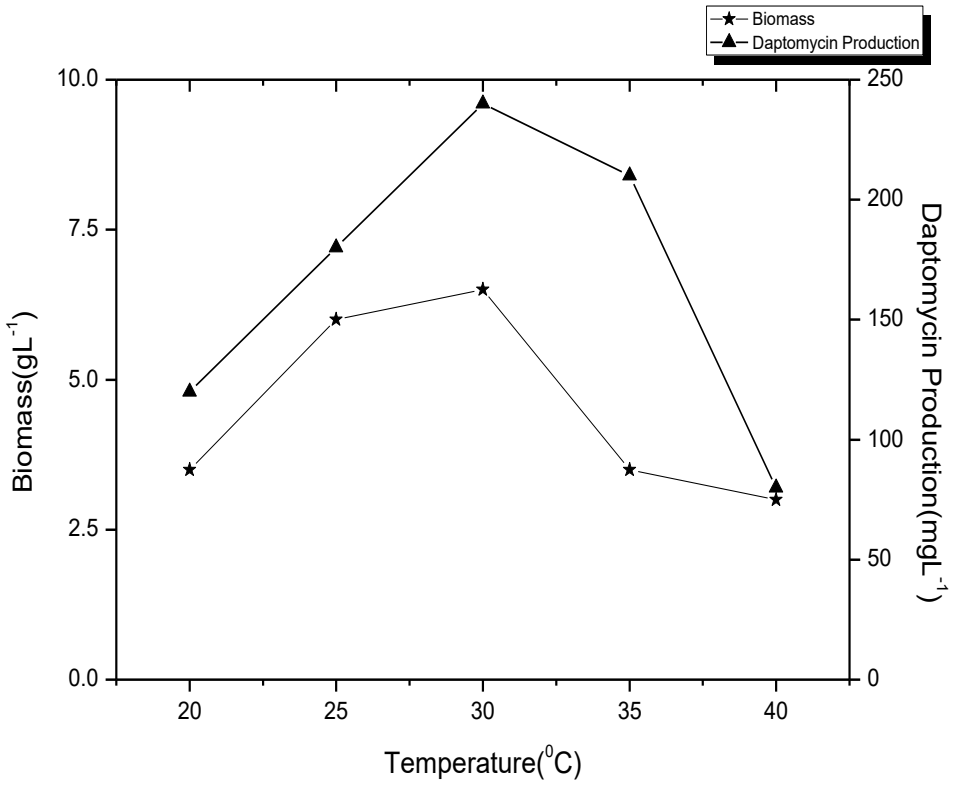

Figure 4.1 Effect of temperature on Daptomycin production

4.1.2 Effect of pH on Daptomycin production

The effect of initial pH on Daptomycin production and the growth of *S. roseosporus* were studied in shake flask containing sterilized fermentation medium by adjusting the pH of the medium in the range of 5-8 at 30°C. The growth of the organism and

Daptomycin titres were measured at 144 hours of fermentation. The pH changes were made steadily. The maximum production was observed at pH 7.0 (230.0 mg/L) which decreased gradually at higher pH. Morphology showed short, swollen and hyphal fragments with fewer arthrospores. The broth became viscous at higher pH. Growth of the microorganism was maximum at pH 6.5 followed by a decline at higher pH. The observed data was shown in graphical form (Figure 4.2).Daptomycin production was most favored by the *S. roseosporus* at pH 7.0 (230.0 mg/L) due to effective metabolic regulation in the stationary phase. At pH less than 7.0, long, slender hyphae with increase in mycelial dry weight were seen. Subsequent fermentations were carried out at pH 7 so as to allow optimum production of Daptomycin and not much reduction in growth.

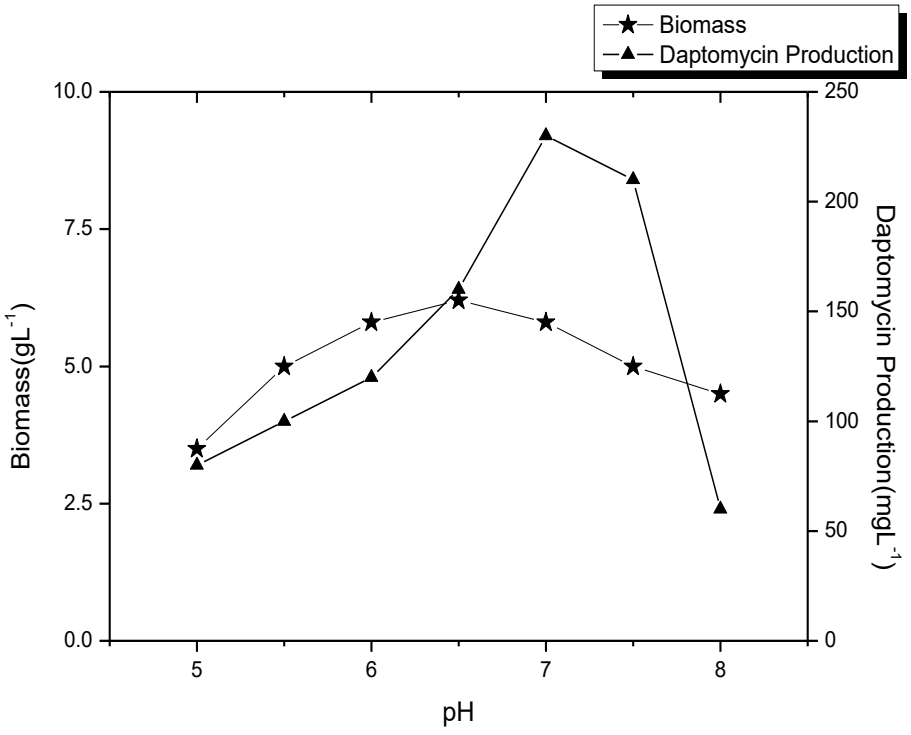

Figure 4.2 Effect of pH on Daptomycin production

The observed data trend is in accordance with literature report of a study [I-Son Ng *et al.*, 2014].

4.1.3 Effect of inoculum age

To study the effect of inoculum age on the Daptomycin production, seed culture of different incubation time ranging from 12-72 h were prepared and allowed to grow in the fermentation medium at 30°C. All the other physical parameters were kept identical as mentioned earlier. The Figure 4.3 shows the effect of different inoculum ages on Daptomycin production.

The maximum production of Daptomycin (240 mg/L) was achieved with the seed culture of 48 h age. As the age of inoculum increased from 12 h to 48 h, increase in the Daptomycin production was observed. The maximum Daptomycin production using 48 h of seed culture was observed and was taken as optimum for further studies. This may be due to the growth profile of the microorganisms entering into the mid-logarithmic phase and further proceeding to the stationary phase of the *S. roseosporus*. Culture age of 48 hours from the seed medium was found most suitable for maximum rate of sugar utilization [Davis *et al.*, 2005].

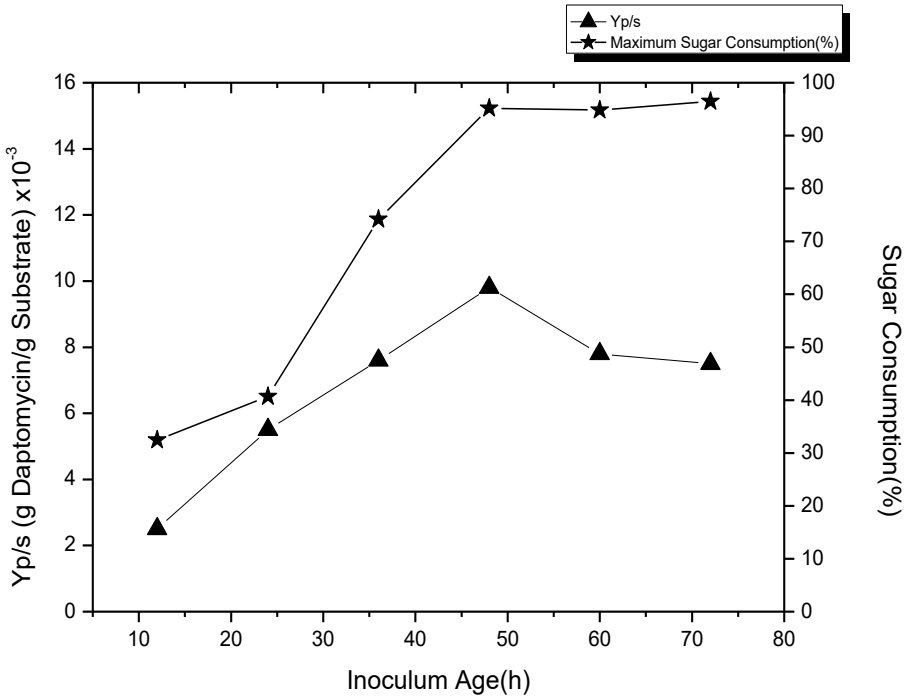

Figure 4.3 Effect of inoculum age on Daptomycin production

4.1.4 Effect of inoculum volume

To evaluate the effect of inoculum volume on the Daptomycin production, different inoculum sizes of the seed medium (2-7% v/v) were inoculated to fermentation medium. All the other physical parameters were kept identical as mentioned earlier. The Figure 4.4 showed the effect of different inoculum volumes on Daptomycin production.

In each run, the maximum yield of Daptomycin and the maximum percentage of sugar consumption were measured. Maximum product yield coefficient ($Y_{P/S}$) was obtained when the inoculum size was 5% v/v. Lower inoculum size (below 5% v/v) did not support the maximum yield of Daptomycin and higher cell volume led to substrate limitation among the cell population[Davis *et al.*,2005]. Both the conditions increased lag

phase. Therefore 5% v/v inoculum level was found to be optimum and was used for further studies. The spore concentration for this volume was found to be $5x10^8$/ml.

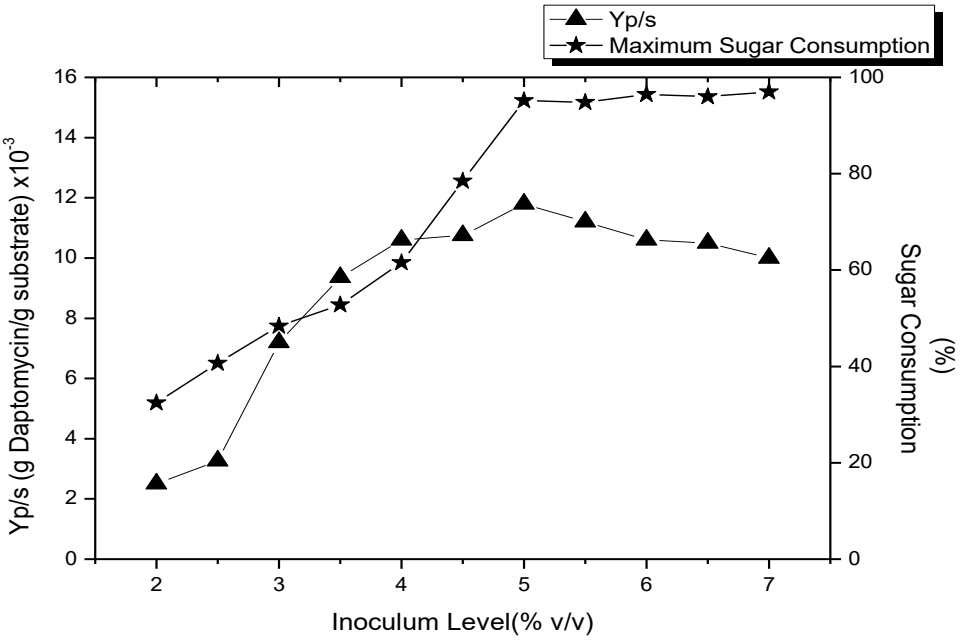

Figure 4.4 Effect of inoculum volume on Daptomycin production

Therefore, experiments were continued using the inoculum size of 5% v/v and above. The results depict the increased yield of Daptomycin and afterwards maintaining a plateau nature. 5% v/v inoculum volume was considered optimum and used in further studies. This may be due to the amount of viable cells present in inoculum supporting maximum growth as well as product yield.

4.1.5 Effect of different carbon sources on Daptomycin production

The effect of different carbon sources on Daptomycin production was shown in Figure 4.5. The dextrin, glucose, sucrose and starch, were considered in the comparison of carbon source. As shown in Figure 4.5, the highest Daptomycin production was achieved

when dextrin was used as the major carbon source. As dextrin belongs to the polysaccharides, it is supposed to be a sequential biodegradation carbon source in cell culture [Saudagar and Singhal *et al*., 2007]. Glucose was indeed suitable except for the fact that it was quickly consumed. Sucrose and starch were appropriate for growth of *S. roseosporus* culture but lacked stimulation for Daptomycin. With reference to previous studies and our experimental assessment, Dextrin was taken as the major carbon source which was degraded slowly along with glucose which was readily consumed and helped in initiating the production process [I-Son Ng *et al*., 2014].

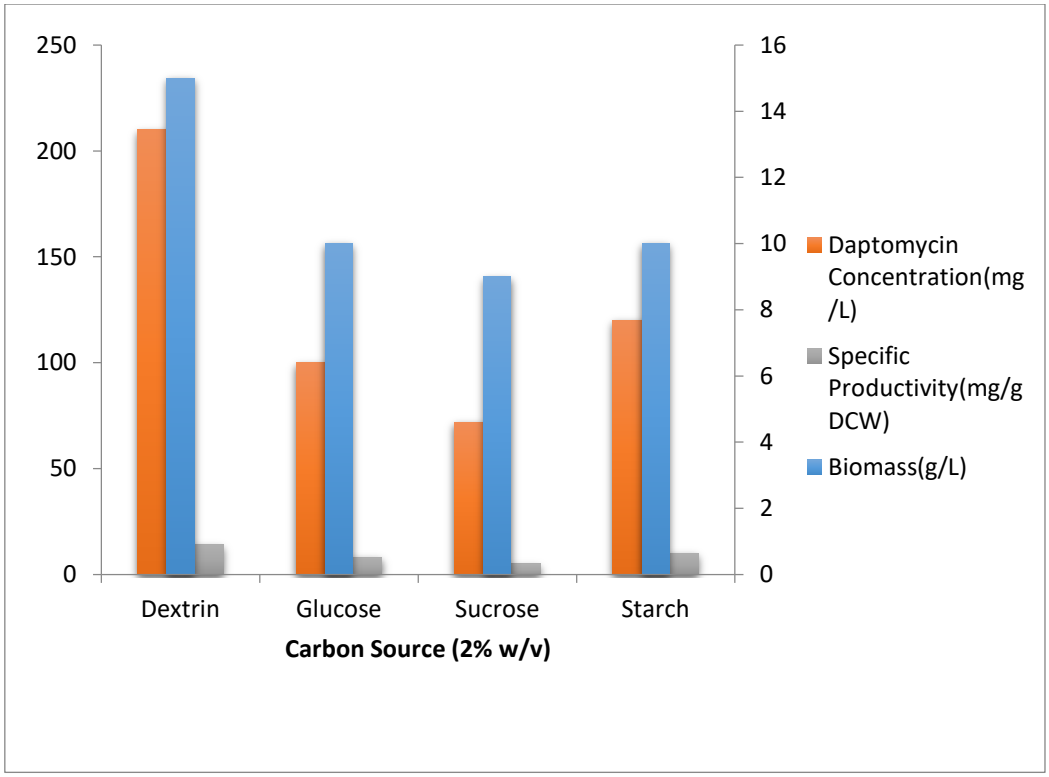

Fig. 4.5 Effect of different carbon sources on Daptomycin production

4.1.6 Effect of different nitrogen sources on Daptomycin production

The effect of different nitrogen sources on Daptomycin production was shown in Figure 4.6. The ammonium chloride, soyabean meal, tryptone, yeast extract, beef extract, sodium nitrite and peptone were considered for the comparison of nitrogen sources. As shown in

Figure 4.6, the highest Daptomycin production was achieved when soyabean meal was used as the major carbon source. Soyabean meal contains several essential amino acids necessary for smooth activities of metabolic pathways involved in Daptomycin production. Similar effect of soyabean flour/meal was seen for actinomycetes species for antibiotic fermentation in previous report [Wei *et al*., 2012]. Among of various nitrogen sources, Soyabean meal was the best as it led to 200.50 mg/L in yield of Daptomycin.

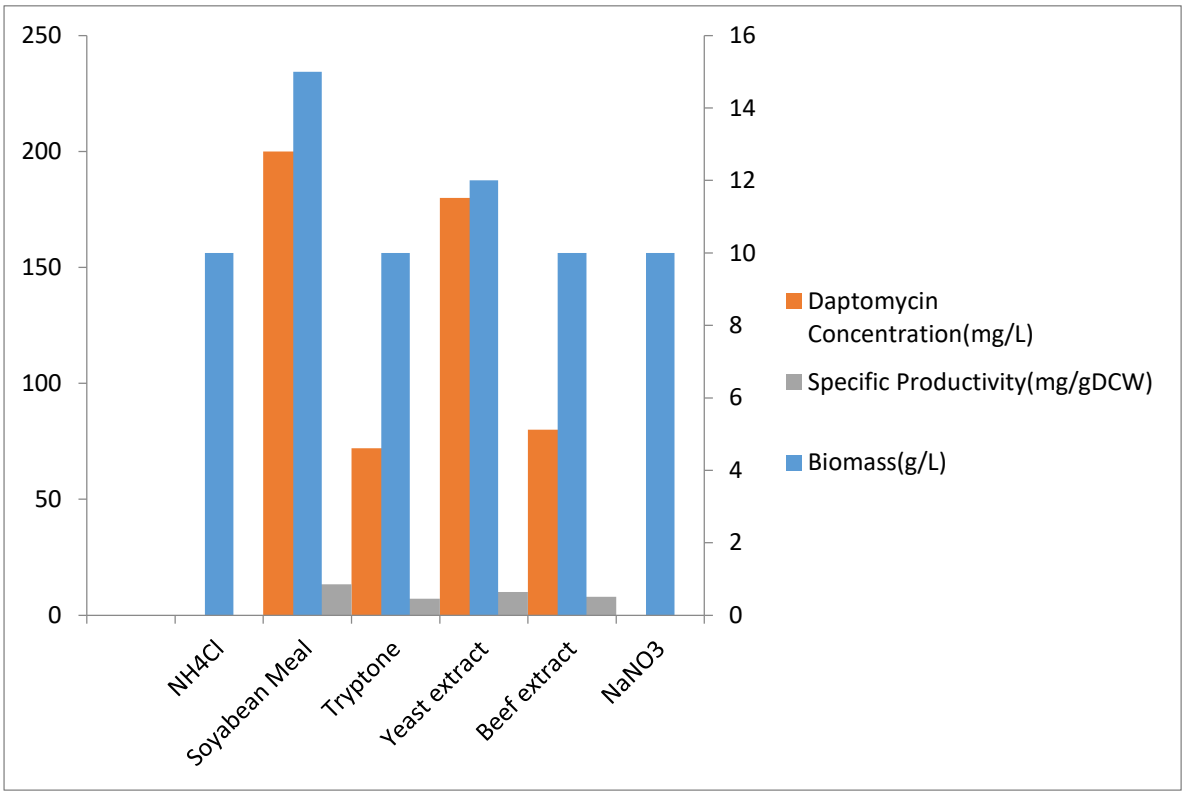

Figure 4.6 Effect of different nitrogen sources on Daptomycin production **(2% w/v)**

4.1.7 Effect of Precursor on Daptomycin production

Daptomycin (cyclic lipopeptide) biosynthesis begins as N-terminus of the exocyclic tryptophan residue is coupled to decanoic acid, a medium-chain (C10) fatty acid. Decanoic acid is the sole precursor of Daptomycin and almost no Daptomycin is produced from *S. roseosporus* without decanoic acid. However, decanoic acid has toxic

effect on the culture of *S. roseosporus*. To address this issue, optimization of the concentration and addition time of decanoic acid was taken care [Lin *et.al*., 2011]. Daptomycin fermentation increased with the addition of decanoic acid from 0.1 to 0.5 g/L. The optimal decanoic acid concentration was found at 0.2g/L for the highest Daptomycin production with sufficient biomass [Holic *et.al*. 2012]. Higher concentrations of this organic acid was poisonous to the cell as the biomass decreased sharply further 0.2g/L. Figure 4.7 (a), Figure 4.7(b) revealed that the addition time of precursor with maximum Daptomycin production was achieved when decanoic acid was added on second day of fermentation. Daptomycin production was not stimulated after the second day. Decanoic acid had an edge over the aliphatic fatty acids for as observed in the case of other lipopeptide antibiotics. The smooth functioning of metabolic pathways for antibiotic biosynthesis ,up-regulated expression of biosynthetic genes rely upon critical time of addition of decanoic acid at 0.2 g/(L day) in the second day after inoculation found to be suitable[Boeck *et.al*.,1990].

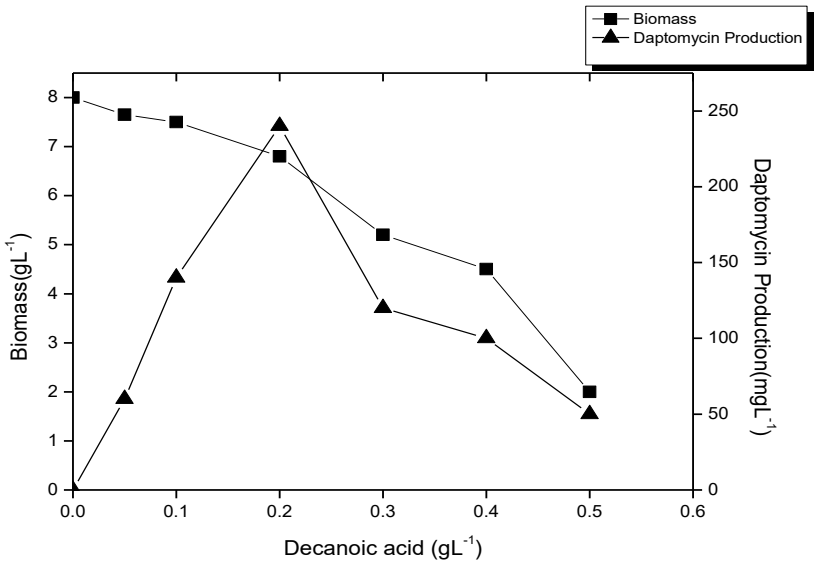

Fig. 4.7 a) Effect of precursor concentration on biomass and Daptomycin production

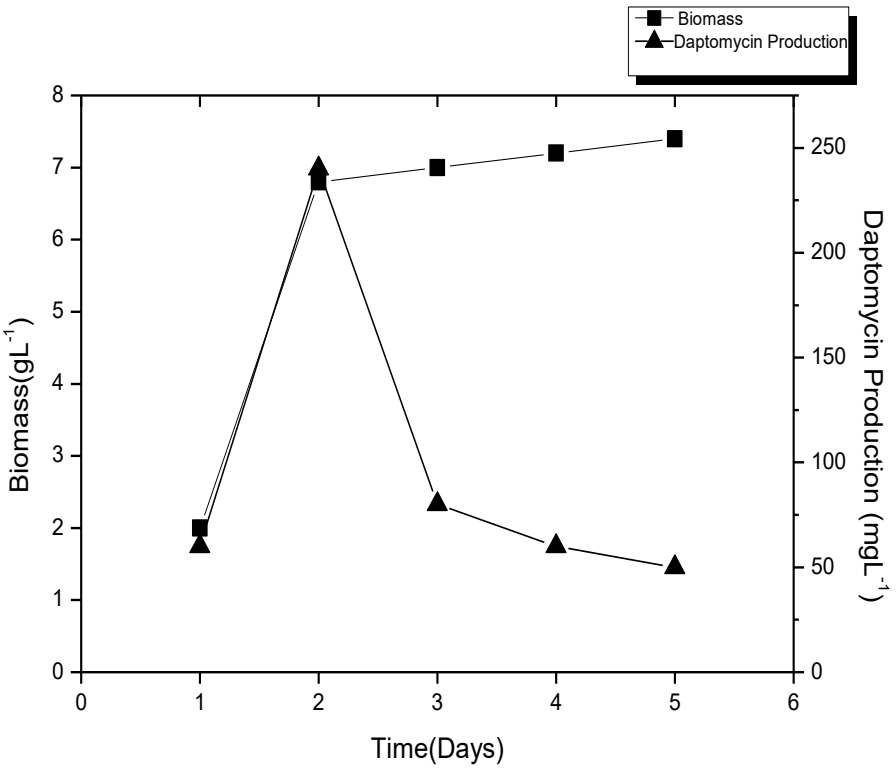

Fig. 4.7 b) Effect of precursor addition time on biomass and Daptomycin production

Decanoic acid was found to be suitable as a precursor for Daptomycin production [Yu *et .al*., 2011]. Further the individual optimum concentration of all these media additives for the maximum Daptomycin production were optimized by the Taguchi Statistical Analysis. After the preliminary method of optimization (OFAT), the results obtained for maximum Daptomycin production are tabulated as following:

Table 4.1: Results of optimization by OFAT method

Culture conditions and media additives	**Optimum Factors**
Carbon source	Dextrin
Supplementary Carbon Source	Glucose

Nitrogen Source	Soyabean Meal
Inoculum age	48 h
Inoculum level	5% (v/v)
pH	7.0
Incubation Temperature	30 °C
Precursor	Decanoic acid, Addition at second day at 0.2 g/l

4.2 Optimization by L16 - Orthogonal Array Method

The media components of Daptomycin fermentation broth were optimized using the L16 - Orthogonal Array Method for their appropriate concentrations. The resultant table of L16 orthogonal array shows the combination of various levels of the variables taken for media formulation. The response of means and signal-to-noise ratio (larger is better) is produced by the L16 orthogonal array and the delta values and ranks for system were noted.

Table 4.2 Results of optimization by Taguchi L_{16} Orthogonal Array

Taguchi L16 Orthogonal Array

Dextrin	Glucose	Soyabean flour	$Fe(NH_4)_2SO_4$	KH_2PO4	**Daptomycin** (mg/L)
1	1	1	1	1	75
1	2	2	2	2	72
1	3	3	3	3	75
1	4	4	4	4	66
2	1	2	3	4	71
2	2	1	4	3	76
2	3	4	1	2	67
2	4	3	2	1	71
3	1	3	4	2	105
3	2	4	3	1	67
3	3	1	2	4	129
3	4	2	1	3	135
4	1	4	2	3	121
4	2	3	1	4	106
4	3	2	4	1	79
4	4	1	3	2	315

Delta values and ranks help to assess which factors have the greatest effect on the response characteristic of interest. Delta measures the size of the effect by taking the difference between the highest and lowest characteristic average for a factor. Higher is the delta value, greater is the effect of that component. Depending on the delta values, rank orders the factors from the greatest effect to the least effect for their response evaluation. The main effect plots for Means and S/N ratios depict how each factor affects the response characteristic.

Table 4.3 Response table for SN ratios and for means

Response Table for Signal to Noise Ratios
Larger is better

Level	A	B	C	D	E
1	37.13	39.15	41.86	39.28	37.25
2	37.05	37.95	38.68	39.51	41.05
3	40.44	38.55	38.86	40.29	39.84
4	42.55	41.53	37.77	38.10	39.03
Delta	5.51	3.58	4.09	2.19	3.80
Rank	1	4	2	5	3

Response Table for Means

Level	A	B	C	D	E
1	72.00	93.00	150.00	95.75	73.00
2	71.25	80.25	89.25	98.25	141.00
3	109.00	87.50	89.25	133.25	101.75
4	156.50	148.00	80.25	81.50	93.00
Delta	85.25	67.75	69.75	51.75	68.00
Rank	1	4	2	5	3

The influence order of the variables was found as Dextrin>Soyabean Meal> KH_2PO4 >Glucose> $Fe(NH_4)_2SO_4$ .Dextrin had a major effect and Fe $(NH_4)_2SO_4$ had least effect on Daptomycin production by *S. roseosporus*. The main effect plots (Figure 4.8) showed how each factor affected the response characteristic. MINITAB software creates the main effects plot by plotting the characteristic average to each factor level. These averages are the same as those documented in the response in Table 4.3.A line connects the points for each factor. When the line is horizontal (parallel to the x-axis), then there is no main effect present. Each level of the factor affects the characteristic in the same way, and the characteristic average is the same across all factor levels. When the line is horizontal (parallel to the x-axis), then there is a minimal main effect present. Different levels of the factor affect the characteristic differently. The greater the difference in the vertical position of the plotted points (the greater the deviation from the parallel x-axis), the greater is the magnitude of the main effect.

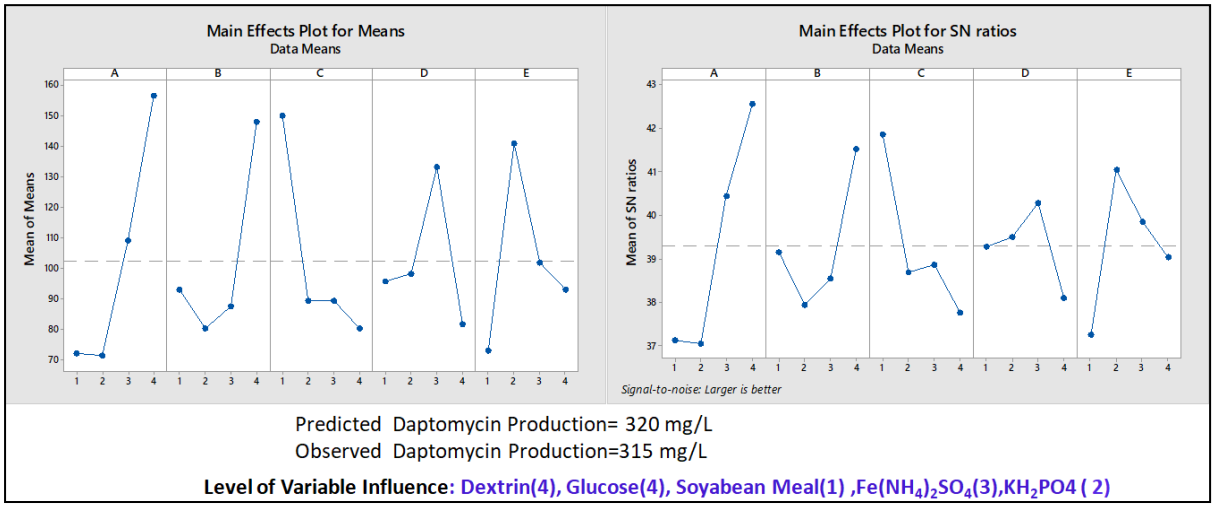

Figure 4.8 Main effects plot for means and SN ratios.

In the present study it can be seen that for each of the four variables at four levels, one level increases the mean compared to the other level [Taguchi, 1986 and Taguchi, 1980]. This difference is a main effect; that is, dextrin at level 4, glucose at level 4, soyabean

meal at level 1, KH_2PO_4 at level 3 and Fe $(NH_4)_2SO_4$ at level 2 show a main effect. These levels also represent the optimal concentrations of the individual components in the medium. From the regression analysis, variables having a P-value of < 0.05 were considered to have a significant effect on Daptomycin production. The results were fitted into polynomial regression model with a correlation coefficient (R^2) of 0.9821.Final medium for Daptomycin production is (g/l), Dextrin 30, Glucose 10, Soyabean flour 20, Fe $(NH_4)_2$ SO_4 0.6 and KH_2PO_4 0.2 and pH 7; incubated at 30 °C for 6 days. To confirm these results, experiments were carried out using these nutrient concentrations, and it was observed that the mean value obtained was 315mg/L as compared to 320 mg/L predicted using MINITAB Version 17 for the same composition. This showed that the experimental value almost matches with predicted values. The final optimized medium produced 315 mg/L of Daptomycin as compared to 200 mg/L before optimization [Bajaj *et al.,* 2009].

4.3 Shake flask studies of Daptomycin production

Daptomycin production was carried out in 500ml shake flasks with 100ml media at the optimized conditions. The biomass production, residual sugar concentration and Daptomycin production profile were generated. The maximum Daptomycin concentration obtained was 350 mg/l. The values of biomass generation, sugar consumption and Daptomycin production were further used to calculate the kinetic parameters.

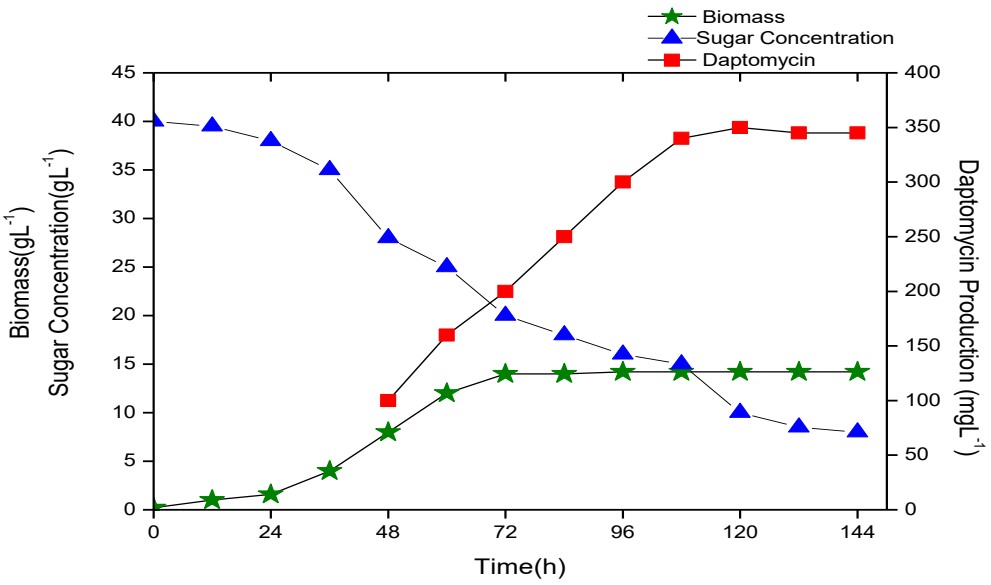

Figure 4.9 Biomass, sugar concentration and Daptomycin production profile in shake flask studies.

The production of Daptomycin started at 48 hours, where the cells entered the mid-exponential phase and reached the maximum production at 132 h. Therefore, Daptomycin production took place in idiophase, which followed the typical pattern of antibiotic fermentation [Kundu *et al.,* 1992]. *S.roseosporus* could accumulate 350 mg/l of Daptomycin within 144 h. The cell dry weight increased sharply till 60 h. But in the last 84 h the microorganism utilized less carbon sources and 8.0 g/l of total carbohydrate concentration was left in the broth at the end of cultivation. It may be attributed to the ability of enzymes that catalyze the synthesis of Daptomycin. The kinetic parameters were then obtained for the values of biomass, Daptomycin production and sugar consumption at different time intervals. The specific growth rate, product formation rate, substrate uptake rate, biomass yield coefficient, growth associated and non-growth associated coefficients of product formation were evaluated. The kinetic parameters were determined using simple rate equation [Doran, 1995]. The specific growth rate of *Streptomyces roseosporus* was found to be $0.0345h^{-1}$and the biomass yield coefficient was evaluated as 0.35 grams of cell mass/grams of substrate. The specific product

formation rate was 0.168 milligrams of Daptomycin per grams of biomass per hour and specific substrate uptake rate was 0.0156 grams of substrate per grams of biomass per hour [Ozergin-Ulgen *et al.,* 1993].

Table 4.4 Table showing various kinetic parameters evaluated for Daptomycin production.

Kinetic Parameters	x_m (Maximum cell mass concentration)	μ_m (Maximum specific growth rate)	$Y_{x/s}$ (Cell mass yield coefficient)	$Y_{p/s}$ (Product yield coefficient)	q_s (Specific substrate uptake rate)	q_p (Specific product formation rate)
Values	14.2 g	0.0345 h^{-1}	0.35 g biomass/g substrate	0.0086 g biomass/g substrate	0.0156 g substrate/ g biomass/h	0.168 mg Daptomycin/ g biomass/h

The cultivation kinetic parameters of batch cultivations indicated clearly that Daptomycin was mainly produced in the stationary phase [Ozergin-Ulgen *et al.,* 1993]. According to this, if the cell activity can be stabilized, the amount of Daptomycin production will increase during the course of fermentation. Higher cell concentration needs to be maintained to enhance the productivity of Daptomycin which is a secondary metabolite of *S.roseosporus* and mainly a non-growth associated product [Li *et al*.,2013]. But, prolonged maintenance of high cell concentration would affect the rheological properties of Daptomycin fermentation. Therefore, rheological characterization of the fermentation broth was done in the succeeding studies [Pamboukian *et al.*,2005].

4.4 Rheological Characterization of Streptomyces roseosporus for the Production of Daptomycin

4.4.1 Morphological changes of *S.roseosporus* during the course of fermentation

After media optimization, the morphological alterations of *S.roseosporus* was studied which influenced the rheology of the broth and hence affected Daptomycin production. The behavior of the microorganism in submerged culture is dictated by several crucial factors like the type of microorganism, media and culture conditions [Huang *et al*., 2011]. The growth of the microorganism and hence the metabolite of interest are greatly affected [Ghildyal, 1987]. On microscopic observation Figure 4.10, three types of morphological forms can easily be observed: freely dispersed long slender smooth filamentous hyphae (up to 48hrs); moderately swollen hyphal fragments (up to 120 hrs) and highly swollen hyphal fragments, unicellular arthrospores (at 144hrs). The maximum rate of Daptomycin production coincides with the differentiation of filamentous hyphae to wide, highly swollen and metabolically active hyphal fragments. A remarkable change was observed in the broth characteristics, after 3-4 days as Daptomycin broth exhibited high viscosity. Morphological variations have often been related to production process in case of many filamentous microorganisms [Matsumara *et al*., 1980].

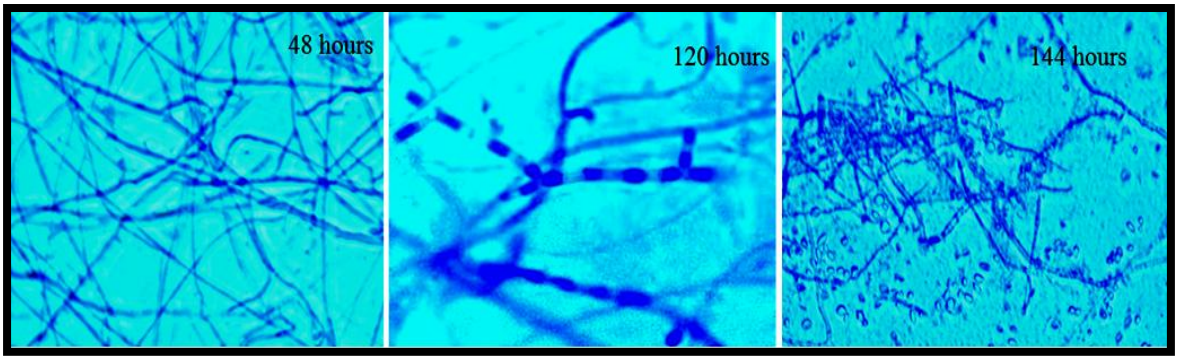

Fig.4.10 Typical morphology of *S. roseosporus* at different time intervals

4.4.2 Rheological properties of the fermentation broth

The pattern depicted as trend of broth rheology clearly showed the non-Newtonian nature of the microbial culture broth. The change in the pattern can be correlated with the differentiation of the microbial cells with the passage of time and the increasing stress conditions. The plots of the shear stress versus the shear rate of culture broths revealed that the culture broth had a non-Newtonian nature and shear stress increased during the course of fermentation. The stress level gradually increased as growth and differentiation of cells took place till the differentiation of hyphal structures into arthrospores.

The shear rate increased abruptly depending upon the shear rate which was dominated by the structural changes of the microorganism. The exponential phase marked by cellular differentiation led to sharp increase in the stress level. Further, different rheological models were plotted to fit the rheological pattern obtained in order evaluate the non-Newtonian behavior of the fluid as shown in Figure 4.11.

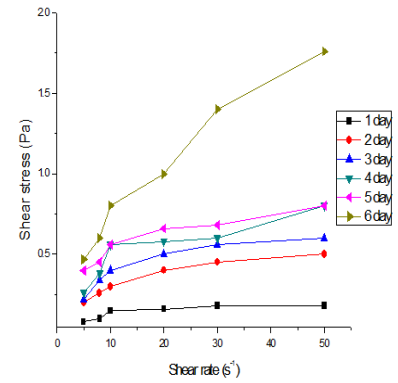

Trend of Broth Rheology

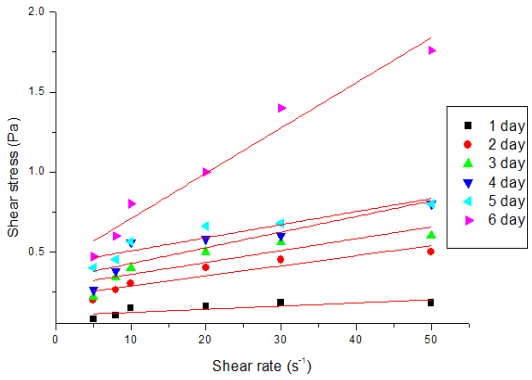

Curve Fitting in Bingham Model

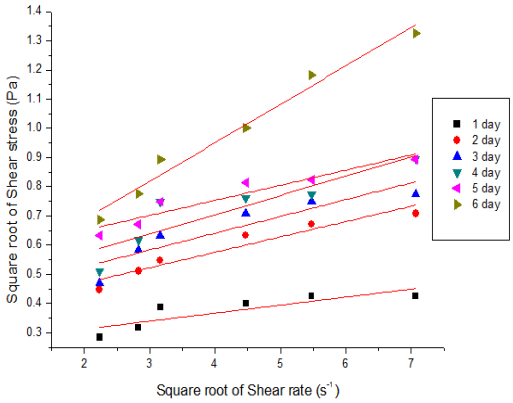

Curve Fitting in Casson Model

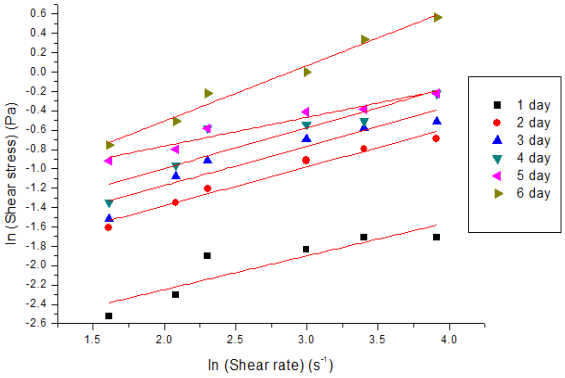

Curve Fitting in Power Law Model

Figure 4.11 Rheological patterns of *S. roseosporus* fitted into different rheological models

Table 4.5 Rheological parameters evaluated for various models

	Power Law Model Parameters			Bingham Model Parameters			Casson Model Parameters		
Days	n	k	R^2	$\tau_{y,B}$	μ_P	R^2	τ	$\mu_{P,C}$	R^2
1	0.6252	0.010	0.8352	0.0015	0.0322	0.782	0.012544	0.000961	0.804
2	0.9034	0.06	0.9431	0.226	0.001	0.9502	0.002809	0.003364	0.947
3	0.5869	0.0619	0.9881	0.1419	0.0097	0.9568	0.057121	0.006084	0.975
4	0.5869	0.0619	0.9881	0.135	0.0097	0.9833	0.142884	0.009025	0.944
5	0.2328	0.2816	0.8638	0.436	0.0054	0.856	0.322624	0.001521	0.833
6	0.5379	0.134	0.976	0.3148	0.0155	0.9006	0.142884	0.009025	0.944

In case of Bingham Plastic Model, the recorded data was predicted by model fitting experiment wherein the Bingham Plastic Model based on linear regression fitted the experimental data well till the fifth day but no evidence of curve fitting was witnessed for sixth day. The parameters obtained from Bingham model and the R^2 values obtained have been sorted in Table 4.5 which reveal that at increased shear rate, the data showed irregular curve fitting. Figure 4.11 represents the shear stress vs. shear rate plots of the culture broths as determined by the Casson model, showing that the Casson model had an edge over Bingham plastic model for prediction of the cultivation of *S.roseosporus*. The parameters obtained from the model and the R^2 values have been depicted in Table 4.5 which show that at increased stress level, the experimental data fitted Casson model better

than the Bingham model.The rheological data fitted the Power law model in the best possible manner and the fitting was better than the other two mathematical models to predict the Non-newtonian behaviour of the broth. The Power-Law model has been quite significant in chemical and biological transport systems. Figure 4.11 have proved that the curves have adapted with the experimentally recorded data fairly well. The parameters obtained from the model and the R^2 values have been represented in Table 4.5 which confirm that the experimental data fits this mathematical model convincingly.

The Power Law model convincingly depicted the rheological patterns of the culture broths of *S. roseosporus* fairly well than the Bingham plastic model. It was also observed that the consistency index (K) and the flow behavior index (n) of the power-law fluid model prompted the morphological variations with increasing stress level demonstrating that the culture broth becomes more shear-thinning with increasing stress.(Figure 4.12). Since, the power law model fitted the data well, the consistency index (K) and the flow behavior index (n) of the power-law fluid model were taken into consideration to show the shear-thinning nature of the culture broth with increasing stress(Figure 4.13).

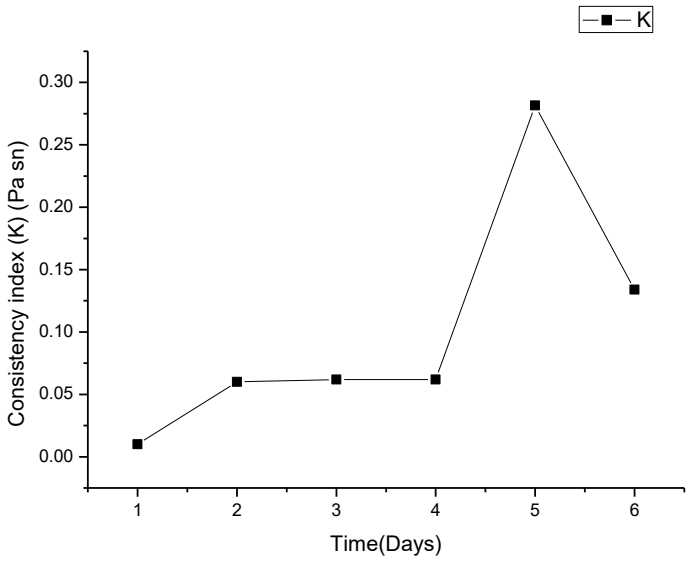

Figure 4.12 Variations in consistency index (K) of Power law fluid model as cell growth occurs

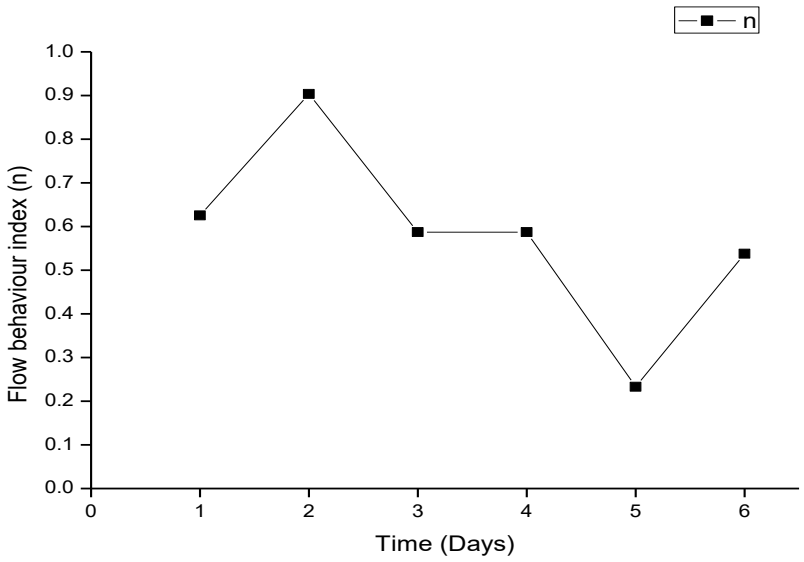

Figure 4.13 Variations in Flow behavior index (n) of Power law fluid model as cell growth occurs

The consistency index (K) for *S. roseosporus* increased and then decreased during the course of fermentation. With increasing stress, culture broth portrayed significant increment in K and n with the passage of time. On the contrary, the power-law index (n) decremented as stress increased, revealing the fact that broth was getting more shear thinning. Such rheological behavior indicated the role of physical and chemical stimulation or enhanced morphological differentiation that demands better mass transfer within the submerged culture [Ghojvand et al., 2011]. The dispersed mycelium network increased the shear stress and shear rate ratio. During the stationary phase, the morphology of *S. roseosporus* was substantially changed in submerged culture , because swollen hyphae in *S. roseosporus* were differentiated in to arthrospores due to the rapid secretion of the antibiotic [Lee et al., 2010]. At low shear stress condition ,the consistency index (K) increased up to 0.28 Pa ·sn on the fifth day and then decreased to 0.13 Pa· sn on the sixth day. This condition was contradicted by the results seen at higher stress condition wherein rapid changes in K and n were revealed. The flow behavior index or the power-law index (n) decreased with increasing stress with the passage of time

indicating the typical shear thinning of culture broth due to complex morphological alterations of actinomycetes [Kumar et al.,2015]. The rheological data changed with the phases of growth of the microorganism. Morphological alterations lead to viscosity of the broth, increased respiration rate and need for proper oxygen mass transfer leading to stress conditions. This stress condition eventually affects the bioprocess or fermentative production of the antibiotic in a negative manner [Alghmadi, 2016]. Therefore, a vivid insight into the rheological pattern of the microorganism would help to track the nature of the fermentative broth and hence to take up measures to increase mass transfer rate through various process strategies.

4.5 Batch Culture Fermentation in a 3L Stirred Tank Fermenter

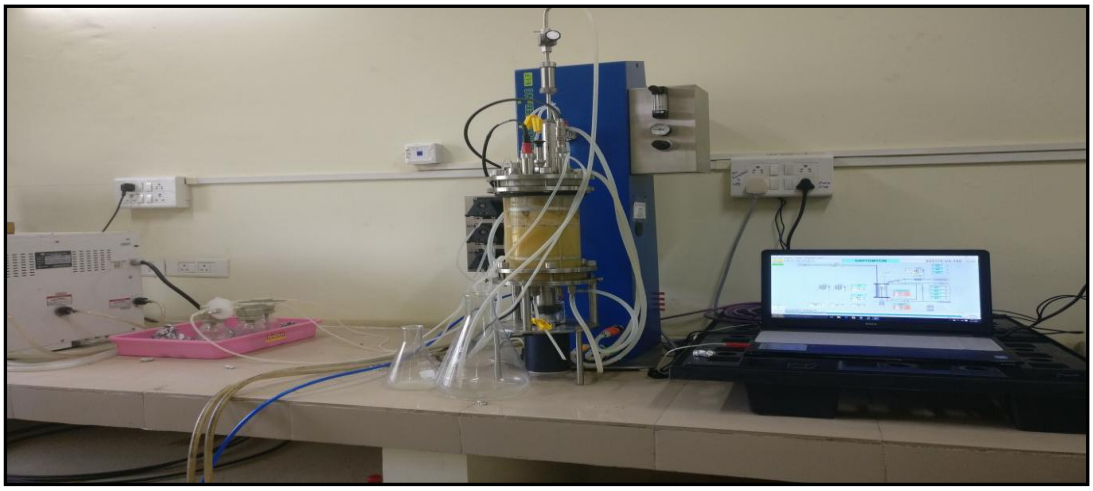

Figure 4.14 Daptomycin productions in a stirred tank bioreactor

4.5.1 Production profile of Daptomycin

Classical fermentation in industry involves batch mode of operation for secondary metabolite production. The commercial production is totally dependent upon the use of free cells in batch, fed-batch or continuous reactors. To optimize the production of Daptomycin, kinetic studies involving fermentation are needed to be carried out. Previous shake flask studies guided the fermentation process in certain limited aspects only. Actual

interpretation of fermentation kinetics was complicated by the ill-defined and ephemeral nature of the environmental conditions in the sequential growth phases. To observe the actual mass transfer taking place in fermenter and the behavior of the culture to produce Daptomycin, fermentation runs were carried out in a 3-L fermenter (Bioengineering, AG) at different physiological states of the culture. The use of stirred culture vessels improves the homogeneity of cultures and allows precise control factors such as pH, aeration and nutrient supply[Nigam *et al.*,2007].

The batch fermentation was initiated by inoculation with actively metabolizing mycelium (5% v/v) grown up in a seed medium. Fermentation studies were carried out under optimum conditions (as determined from shake flask studies) in a 3L fermenter. Two separate profiles were obtained. One for the growth of the organism and the other for Daptomycin production. Maximum Daptomycin titre was obtained as 568 mg/L while the maximum growth obtained was 18g/L. The antibiotic, Daptomycin, is produced at its maximal rate after an initial period of rapid growth of the microorganism [Srivastava *et al.*,1995,1996].Like Gaden class IIII fermentation kinetics idiophase and tropophase were clearly distinguishable. There is an inverse relationship between specific growth rate and specific product formation rate. The graphs clearly depict that Daptomycin is mainly a non-growth associated product [Gaden,1959].

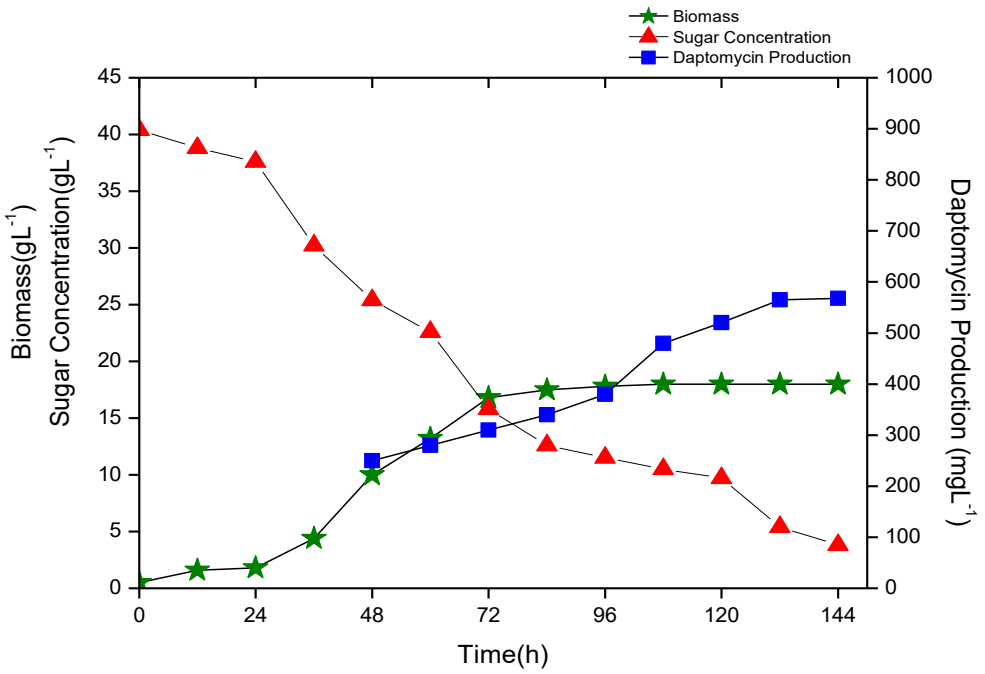

Figure 4.15 Daptomycin production profile and biomass with respect to time course of Daptomycin production

4.5.2 Aeration and agitation in Stirred tank bioreactor

Batch fermentations were carried out at varying air flow rates ranging from 1 vvm to 3.5 vvm while maintaining constant agitation at 400rpm and 600 rpm. K_La was computed at various air flow rates as shown in Figure 4.16. Daptomycin production was found to be optimum at an air flow rate of 2.5 vvm corresponding to the K_La value of 40 h^{-1}. Above this flow rate, K_La was increasing but production was almost constant. There is no effect of volumetric oxygen transfer coefficient above a critical value on the production of Daptomycin indicating attainment of DO saturation for *S.roseosporus*. In case of agitation without any aeration the minimum oxygen transfer coefficient was $8h^{-1}$transfer which means that the liquid film resistance was high. The Daptomycin production and K_La was more for 400 rpm than 600 rpm. At higher rpm, shear sensitivity of the cells was affected.

S.roseosporus cells were damaged and viscosity increased in the broth. This adversely influenced the Daptomycin production as well as the volumetric oxygen transfer coefficient [Wang *et al.*,2007]. Volumetric oxygen transfer coefficient is a very important factor in Daptomycin biosynthesis process as it is an aerobic system's product and requires oxygen right from its initiation step[Tally and De Bruin 2000; Robbel and Marahiel 2010].

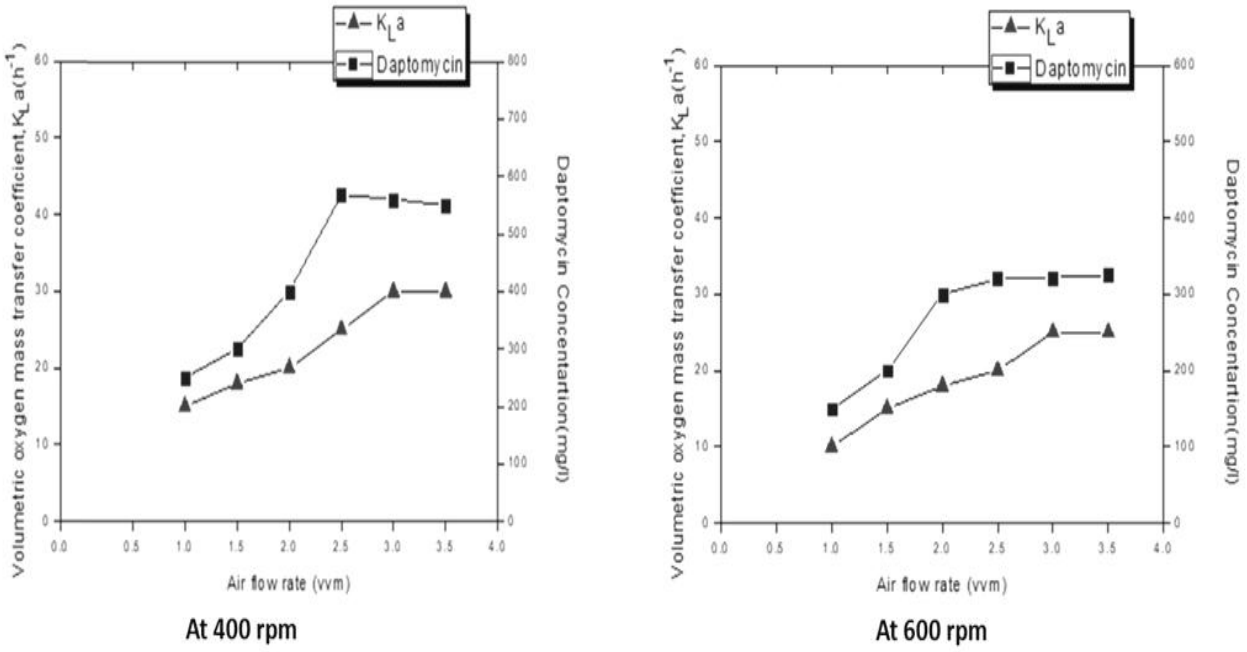

Figure 4.16 Daptomycin production and volumetric mass transfer coefficient with respect to aeration and agitation.

For effective oxygen mass transfer, gas sparging was necessary to break the liquid film resistance. Volumetric mass transfer coefficient decreased with increasing time of fermentation. This observation was attributed to the change in morphology of *S.roseosporus* and increased viscosity therefore. The long slender hyphae swell gradually during idiophase and ultimately decompose to form arthrospores. Predominance of

arthrospores during idiophase increase markedly the broth viscosity observed during late stages of fermentation while long and slender dominate tropophase[Sousa *et al.*,2002;Mishra *et al.*,2005].

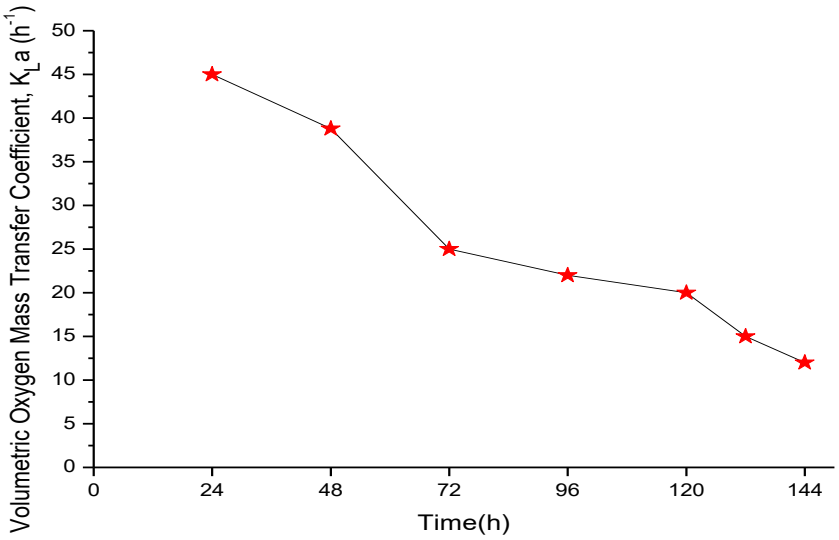

Figure 4.17 Volumetric mass transfer coefficient with respect to time profile of Daptomycin production

4.6 Continuous Production of Daptomycin in a Packed Bed Bioreactor using *Streptomyces roseosporus* by novel immobilization techniques

4.6.1 Effect of cells to carrier ratio

The proportions of different immobilization materials viz., loofah sponge, silk sachet and calcium alginate bead were varied with cell concentrations. Six different ratios of microbial cells to carrier varying from 0.5 to 3.0 grams of cell mass per gram of carrier were used for immobilization and were packed in the bioreactor. Daptomycin production and cell leakage were estimated and analyzed for each ratio. The extent of cell leakage and the ability of the immobilized cells in the production of Daptomycin are shown in Figure 4.18 and Figure 4.19. The Daptomycin production and the cell leakage were

maximum for natural loofah sponges i.e. 1230 mg/l and 200 mg/l respectively. The pattern of antibiotic production was lower for silk sachets and calcium alginate beads as compared to natural loofah immobilized cells. However, the cell leakage was predominant in natural loofah sponges in comparison to other immobilizing agents. Higher cell concentration can be maintained by immobilization methods which enhance the productivity of this antibiotic as it is mainly a non-growth associated product. Prolonged reusability is also an advantage of whole-cell immobilization [Srivastava and Kundu 1998; Nigam *et al.*, 2005]. These characteristic properties of whole cell immobilization were harnessed to get enhanced production of Daptomycin in a packed bed bioreactor run in a continuous mode. Three different immobilization techniques were applied. Natural loofah sponges were used as adsorbents immobilization mode while calcium alginate beads and silk sachets were used for cell entrapment immobilization mode. Two significant factors were optimized to evaluate the production of Daptomycin over the time. The first factor was cells to carrier ratio. The proportions of the grams of cell biomass and support materials were varied and the production of Daptomycin was observed in each case. Daptomycin production profile depicted a distinct peak which rose up to a particular ratio then declined considerably. With the increase in cells to carrier ratio, there was a regular increase in cell leakage. This characteristic feature of each immobilization mode was due to the fact that at lower ratios, the mass transfer of the substrate was not hampered whereas at higher ratios, cell leakage was dominant thereby eventually reducing biomass and leading to the decline in antibiotic formation[Zhang *et al*., 2013]. A cell to carrier ratio 3:2 was found to be suitable for maximum Daptomycin production after which the production declined. Another interesting phenomenon was noted. Though cell leakage was more pronounced with loofah sponge as compared to the other two immobilization methods, yet Daptomycin production was eventually maximum

for loofah sponge. This observation can be attributed to the potential mass transfer barrier which hampered the production in case of silk sachets and calcium alginate beads but was recessive in case of loofah sponges [Goosen *et al.*,1999].The porous network of loofah sponges gave enough space for filamentous cell growth. The increased production of Daptomycin in immobilized system over free cells was accounted due to changes in permeability of cell walls and reusability of the matrices (Morikawa et al., 1979; Chakravarty et al., 2016).

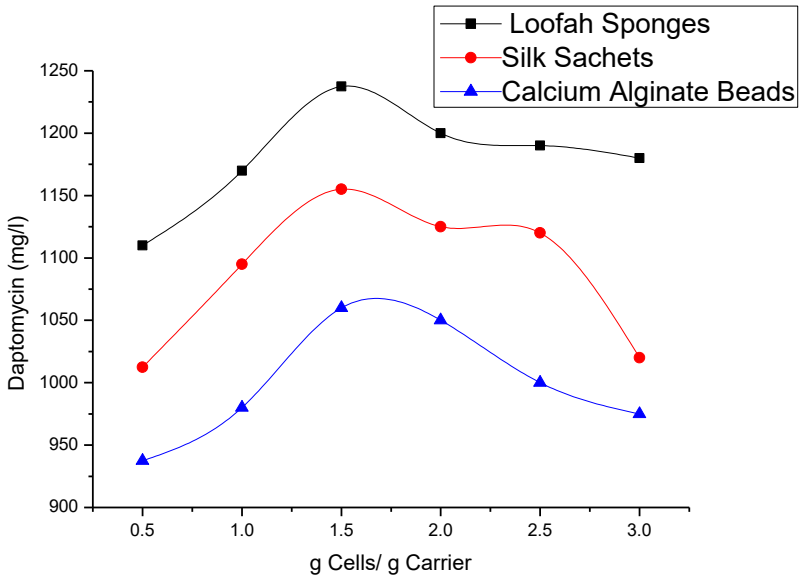

Fig. 4.18 Daptomycin productions for different ratios of cells and carriers.

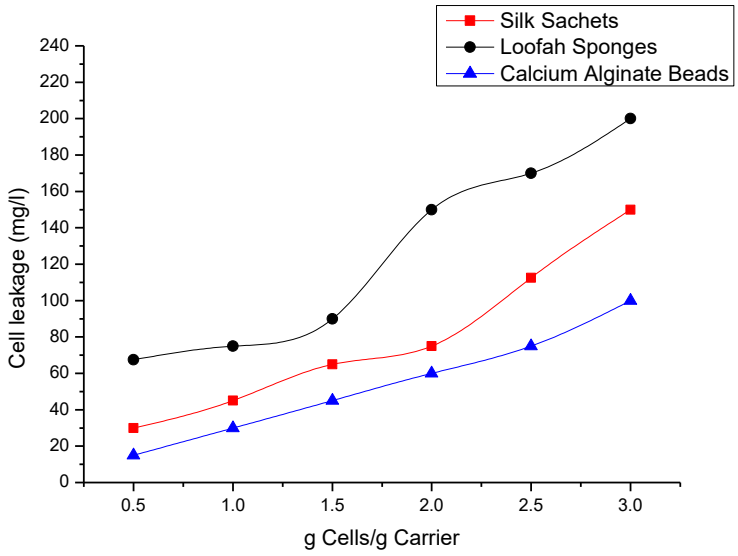

Figure 4.19 Cell leakage Profiles for different ratios of cells and carriers.

4.6.2 Effect of Dilution rate on Daptomycin production

The Dilution rate in the packed bed bioreactor was varied from 0.01 h^{-1} to 0.040 h^{-1} and the output samples of product and unused substrate were collected and analyzed. The Daptomycin production, substrate consumption and overall Daptomycin productivity were investigated for each dilution rate as shown in Fig.4.20 to Fig. 4.22. Daptomycin production was more for lower dilution rates. It increased with the decrease in the dilution rate because of longer residence time inside the bioreactor. After reaching a certain dilution rate, fall in Daptomycin production is rather sharp, indicating that upto a critical residence time, the production was maximum and after that issues like mass transfer of substrate might influence production (Singh et al., 2014). The residual sugar concentrations reveal the issues of mass transfer limitation at higher dilution rates and that the sugar utilization was better for natural loofah sponges than other two immobilization modes. Antibiotic production was highest for loofah sponge 1240 mgl^{-1}

followed by silk sachets 1160 $mgl^{-1}$and calcium alginate beads 1000 mgl^{-1}. The substrate consumption increased with the passage of time for each immobilization mode. The optimal dilution rate was found to be 0.025 h^{-1} where the productivity (Dilution rate multiplied by Product formation) was observed to be maximum for each of the immobilization mode. It was 29.5 mgL^{-1} h^{-1} for natural loofah sponges followed by 25 mgL^{-1} h^{-1} for silk sachets and 21.25 mgL^{-1} h^{-1} for calcium alginate beads immobilized cells. It is known that in case of free cells, as Dilution rate increases, substrate consumption increases slowly in the beginning and then more rapidly as Dilution rate approaches to maximum specific growth rate value (μ_{max}); also, product formation decreases as cell biomass approaches to zero; Dilution rate tends to maximum specific growth rate (μ_{max}). The condition at higher dilution rate whereby cell biomass reduces to zero is known as washout phenomenon. Washout of cells occurs when the rate of cell removal in the bioreactor outlet stream is greater than the rate of cell mass generation and product formation. To avoid such condition for packed bed run in continuous mode, the operating dilution rate is kept at less than μ_{max} value. Close to washout, the system is very sensitive to small changes in Dilution rate which causes relatively large shifts in product formation and substrate consumption. Therefore, the optimization of Dilution rate plays an important role in this system. However, in the present work, immobilized-cells in continuous mode of cultivation could be operated at Dilution rate upto 0.04 h^{-1}, considerably higher than average μ_{max} (0.028 h^{-1}) of immobilized cells.

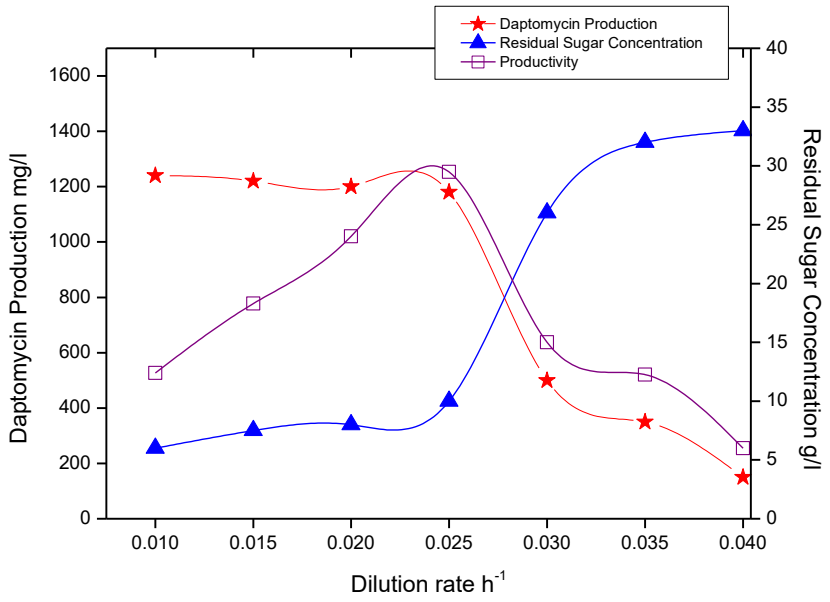

Figure 4.20 Daptomycin production, residual sugar concentration and Daptomycin Productivity Profiles for Natural Loofah Sponge varying with different Dilution rates**.**

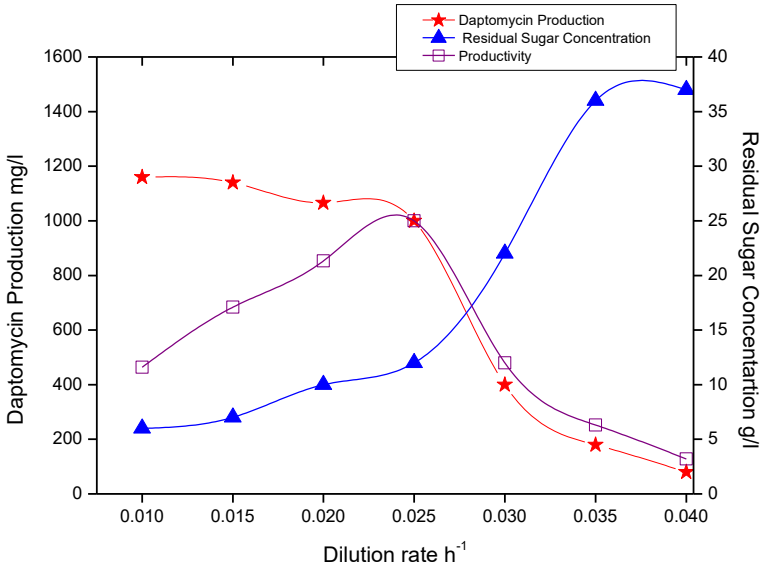

Figure 4.21 Daptomycin production, residual sugar concentration and Daptomycin Productivity Profiles for Silk Sachets varying with different Dilution rates.

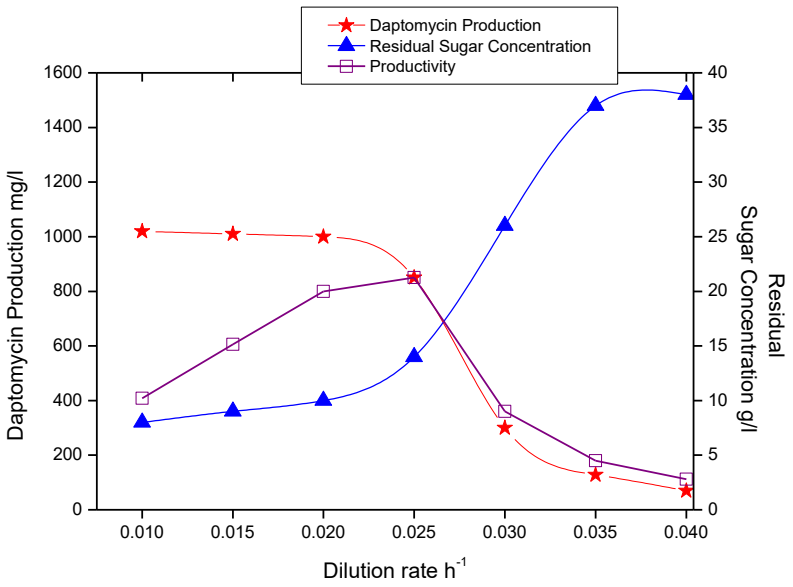

Figure 4.22 Daptomycin production, residual sugar concentration and Daptomycin Productivity Profiles for Calcium Alginate Beads varying with different Dilution rates.

At the given dilution rate, utility of immobilized cells improved substrate utilization and reduced the amount of substrate lost in the product stream. In fact, decreased rate of reaction with immobilized cells at higher D value were caused due to the effects of mass transfer resistances in and around the support carriers. Therefore, at maximum dilution rate, 0.04 h^{-1} the production was minimized but complete washout was not observed. There was a significant shift in the washout tendency and the residence time was prolonged (Doran, 1995). The maximum productivity was accounted at a dilution rate of 0.025 $h^{-1}$for all the three immobilization methods. Natural loofah sponges gave higher Daptomycin production and productivity than silk sachets and calcium alginate beads. This response was in sync with the results obtained earlier with different ratios of the carrier materials.

4.6.3 SEM images of immobilization matrices

S.roseosporus cells immobilized on Loofah Sponge, Silk Sachets and Calcium alginate Beads were studied by scanning electron microscopy. The SEM photograph showed the pore distribution of the carrier matrix as seen in Figure 4.23.The Scanning Electron Microscopic photographs show the inner pores of carriers used. The porous network shown in the SEM images clearly reveal the surface texture, topology and morphology of the microbial cells (adsorbed/entrapped in the support material) and the adsorbent and entrapment materials [Ghali *et al.*, 2009]. The present study confirmed that Daptomycin production with whole cell immobilization strategy in a packed bed bioreactor showed improved results. Therefore, whole-cell immobilization can be considered as an important strategy for improved production of this useful antibiotic/ drug.

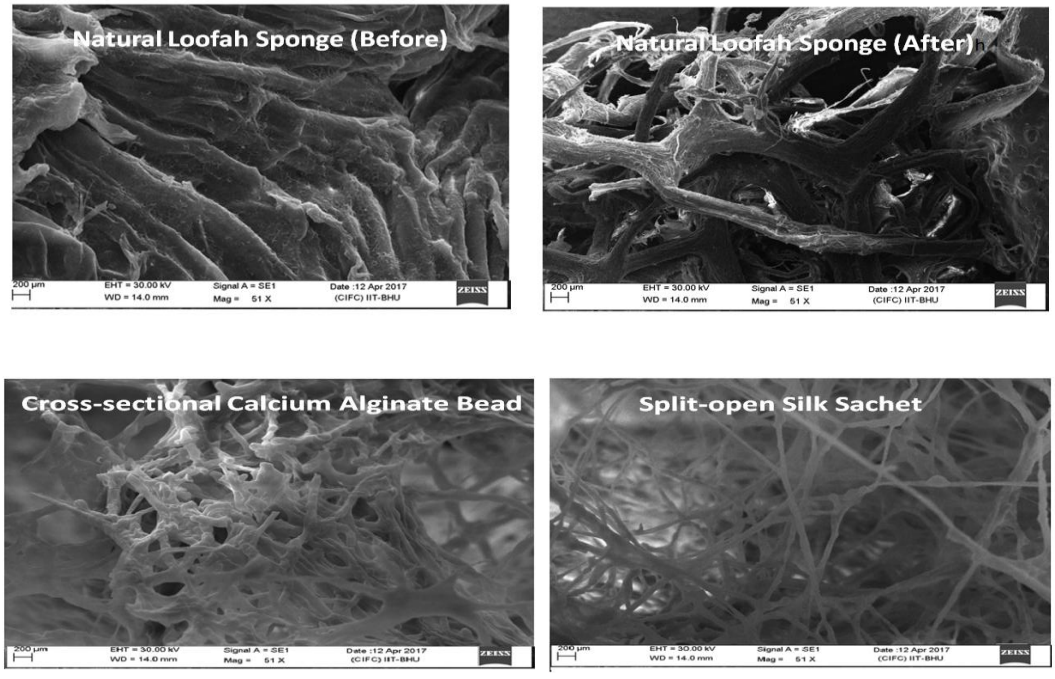

Figure 4.23 SEM images of the cross-section of different immobilization materials used in a packed bed bioreactor.

4.7 Daptomycin production in an airlift bioreactor by morphologically modified and immobilized cells of *Streptomyces roseosporus*

4.7.1 Preliminary screening of support matrices

The significance of whole cell immobilization was evaluated by screening five different conventional and non-conventional support matrices viz., ultra porous refractory brick flakes, silk sachets, polyurethane foam, loofah sponge and ceramic foam as shown in Figure 4.24. The reusability, retention capacity, immobilization time, mechanical stability and economic viability prompted the use of refractory bricks and silk sachets. Since, airlift bioreactor was used, buoyancy and repeated utility of the matrix was taken into consideration. BET analysis was done to determine the characteristics of the refractory brick referred in materials and methods.

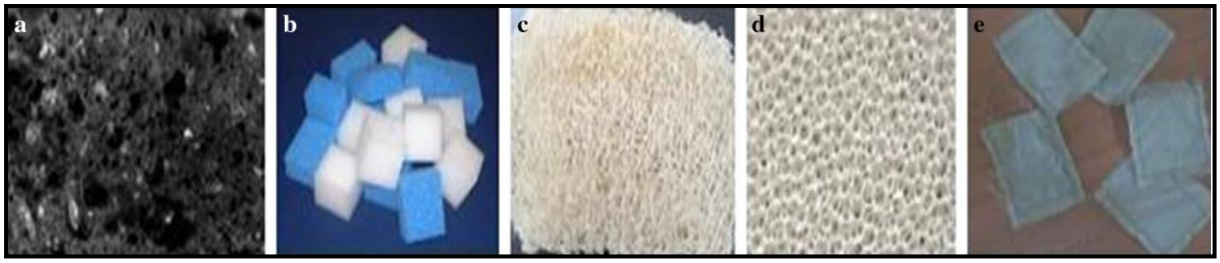

Fig. 4.24 Different immobilization materials screened. **a** Ultra porous refractory brick, **b** polyurethane foam, **c** loofah sponge, **d** ceramic foam, **e** silk sachets

4.7.2 Effect of different parameters (viz. nitrogen sources, inoculum size and aeration rate) on pellet formation

The morphological variation of *S. roseosporus* was carried out by changing the inoculum size, the nitrogen source and reducing aeration rate in the fermentation medium as shown in Table 4.6.

Table 4.6 Optimization of various conditions for pellet formation.

Air flow rate = 0.70 vvm		
Nitrogen Source	Inoculum size	
	4% (v/v)	5% (v/v)
Soyabean meal	Entangled mycelia filaments	Dispersed mycelia filaments
Peptone	Small and smooth pellets	Small irregular mycelial clumps
Yeast extract	Big and fluffy pellets	Entangled mycelial clumps

Several visual differences were observed in terms of the branching of hyphae and hyphal arrangement (Figure 4.25).

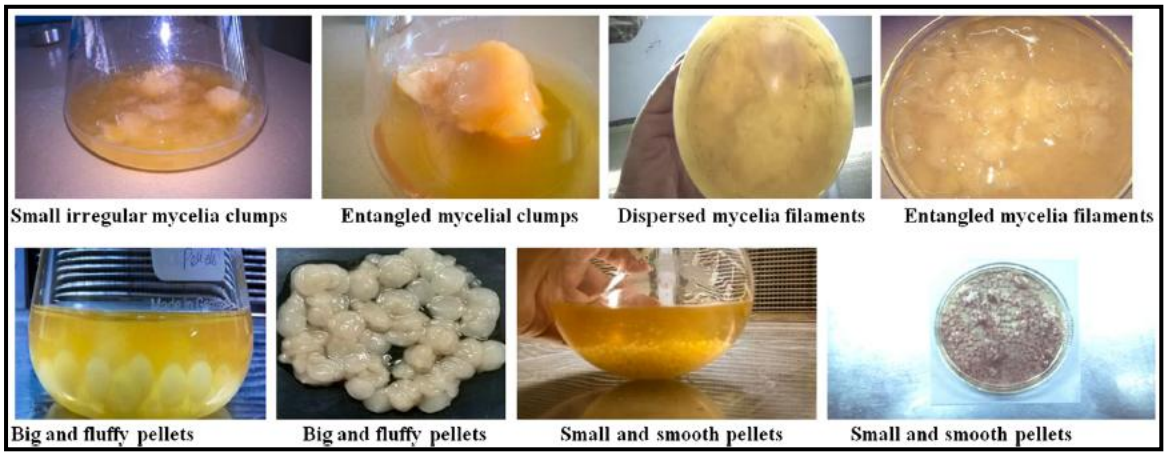

Fig. 4.25 Morphological variations of *S.roseosporus* with different growth conditions.

The filamentous nature of actinomycetes leads to its shear-sensitivity. Therefore, airlift bioreactor was chosen. Daptomycin production with free cells, pelletized cells and immobilized cells on various support matrices depicted the correlation of morphological

variations with antibiotic production. The production of Daptomycin by immobilized cells was compared with that of two morphological forms of the cells i.e. free and pelletized cells. Two types of pellet growth occurred in media using peptone as nitrogen source and yeast extract at 4% inoculum size. Smaller pellets formed by peptone supplemented media with 4 % (v/v) inoculum were more advantageous for antibiotic production due to their high surface to volume ratio [Nielsen *et al.* 1995]. Faster consumption of peptone as a nitrogen source and low inoculum size led to comparatively slower growth of cells and nitrogen starvation. The cells started utilizing cellular nitrogen leading to stress conditions. *S. roseosporous* is a strict aerobe. It is necessary to provide sufficient dissolved oxygen during the fermentation. The dissolved oxygen tension in bulk fluid was increased by lowering the air flow rate to 0.70 vvm which led to high oxygen tension on the surface and in the centre of the pellets. Previous literature(s) support that improving DO tension in submerged cultivations is favorable for the pellet formation, as described in [Du *et al.* 2003].

In the beginning, Daptomycin production was evaluated using free cells in the internal loop airlift bioreactor. Figure 4.26 depicts the profiles for biomass, Daptomycin production and residual sugar concentration at different time intervals upto 144 hours in a single run using free cells, Daptomycin production was accounted as 750 mg/l for a maximum biomass 18 mg/l. The free cells were appropriate for a single run only. Although the production in airlift bioreactor was considerably good as there was no agitation and shear sensitivity of cells were taken care of with improved aeration.

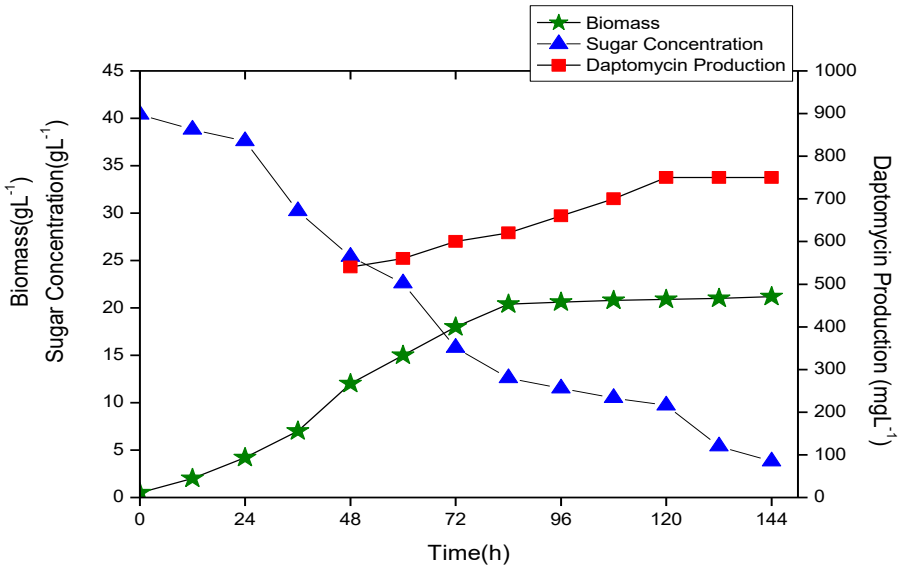

Figure 4.26 Daptomycin production profile in an airlift bioreactor (using free cells).

The data of Daptomycin production for free cells of *S.roseosporus* was compared with that of stirred tank bioreactor (Figure 4.15). Though dry cell weight was not hampered much in case of stirred tank bioreactor when compared with airlift bioreactor results as it included both live and ruptured cells but there was a significant difference in Daptomycin production in case of these two reactors. The differences in Daptomycin production,specific growth rate and Daptomycin productivity are shown in Table 4.7.

Table 4.7 Comparisions between Daptomycin production in an internal loop airlift bioreactor and that in stirred tank bioreactor.

S.No.	Parameters	Bioreactor	
		Internal Loop Airlift Bioreactor	Stirred Tank Bioreactor
1	Working volume	1.5 L	2.0 L
2	Maximum Biomass	18.0 gL^{-1}	15.0 gL^{-1}
3	Daptomycin	750 mgL^{-1}	568 mgL^{-1}

4	Specific growth rate (μ)	0.045 h^{-1}	0.040h^{-1}
5	Daptomycin Productivity	5.2 x 10^{-3} $gL^{-1}h^{-1}$	3.94 x 10^{-3} $gL^{-1}h^{-1}$

4.7.3 Correlation of cell morphology and Daptomycin production

The production profile of immobilized cells revealed that the antibiotic production started at 48 h of fermentation with immobilized cells on refractory bricks and reached maximum level (700 mg/l) by 144 h. On further incubation, no improvement in antibiotic production was observed. In case of free cell fermentation, the maximum antibiotic production (750 mg/l) was observed by 144 h as shown in Figure 4.21.

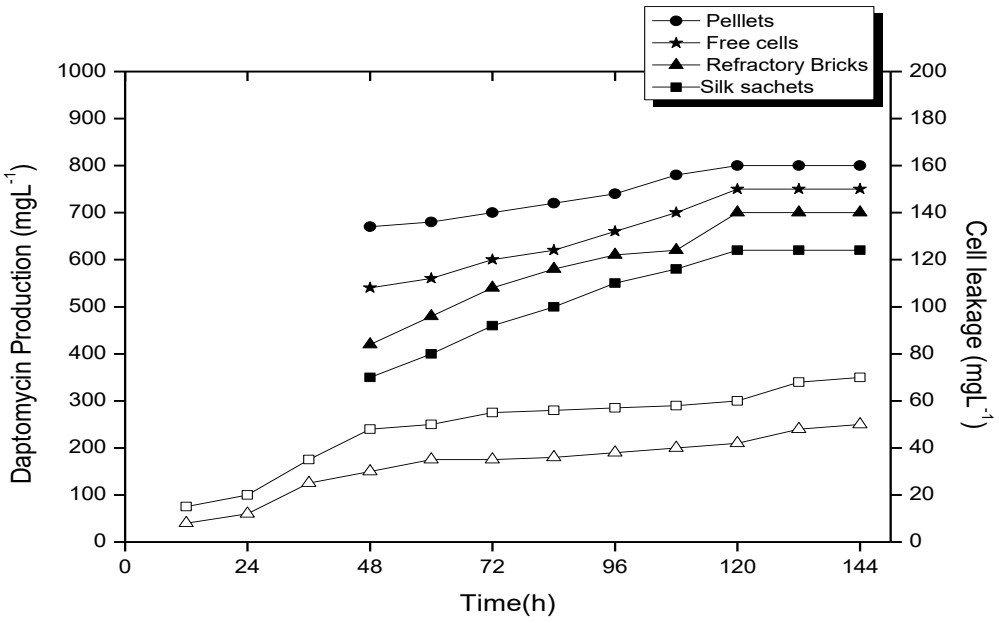

Fig. 4.27 Profiles for Daptomycin production using different modes of cells and cell leakage- free cells, pelletized cells, immobilized cells on refractory bricks and immobilized cells on silk sachets.

The Daptomycin production profile (Figure 4.27) with immobilized cells on silk sachets indicates a progress in cell mass and antibiotic titre up to 144 h. The maximum antibiotic yield with immobilized cells on silk sachets reached 620 mg/l. Small and fluffy cell pellets were utilized for Daptomycin production. The growth and Daptomycin production profiles with pellets indicate progress in cell mass and antibiotic production up to 144 h. The maximum antibiotic yield with pellets reached 810 mg/l.

4.7.4 Reusability of cells pelletized and immobilized cells

Repeated batch fermentation process was carried out for Daptomycin by *S. roseosporus* cells immobilized on refractory brick and silk sachets as shown in Figure 4.28.

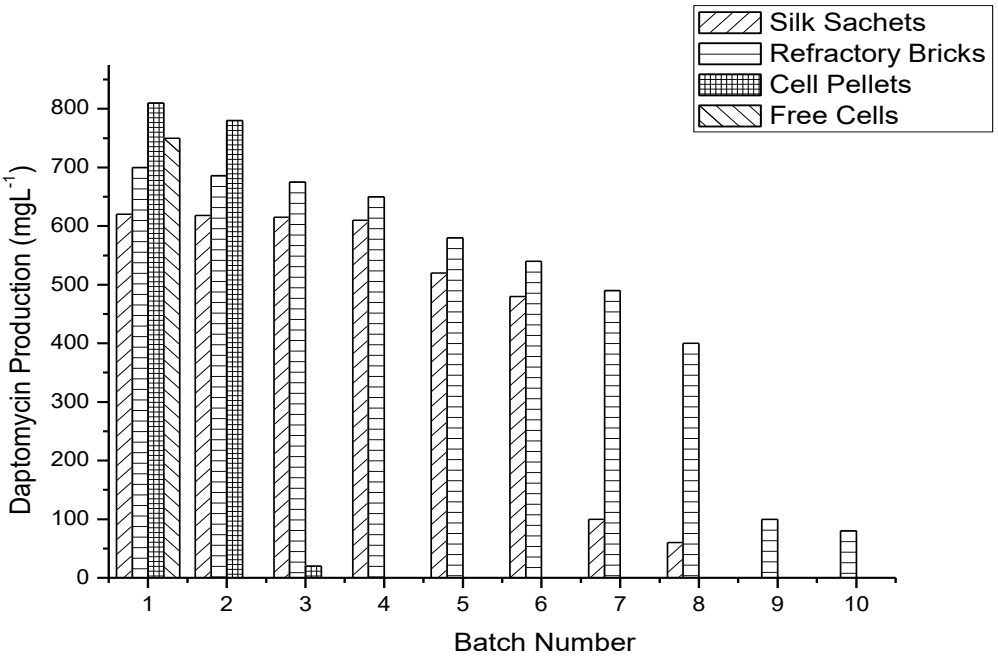

Fig 4.28 Repeated batch fermentation with *S.roseosporus* cells in different modes.

These modes were found to be superior due to low cell leakage and stable for repeated use. Significant process engineering advantages are evident from immobilized cells in

repeated batch operations. Reusability of immobilized cells was achieved by aseptic removal of fermentation medium and replacement with afresh medium for *S. roseosporus* production. Daptomycin production was studied up to ten reuse cycles. The fermentation was continued for several batches until the carrier material disintegrated. There was an increase in Daptomycin production up to eighth cycle for refractory brick immobilized cells and later a gradual decrease in antibiotic production was noticed. Similarly, for the silk sachets, the production could be repeated for six cycles.

4.7.5 Microscopic view of different cell morphology

Streptomyces roseosporus cells as free cells and immobilized cells were studied by electron microscopy. The SEM photograph showed that cells were randomly distributed in the pores of the carrier matrix as seen in Figure 4.29.

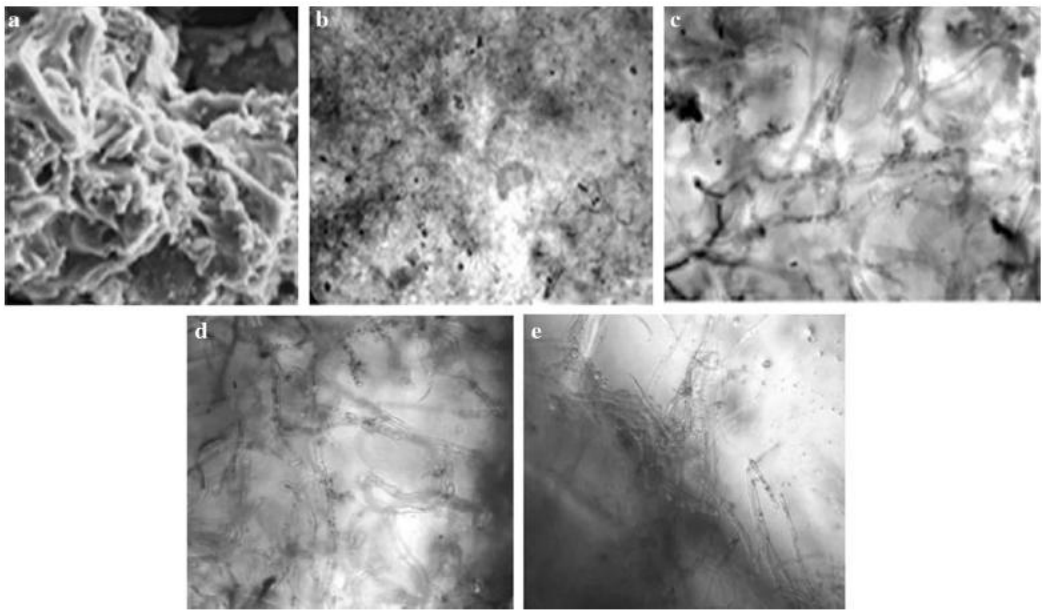

Fig. 4.29 Microscopic view of S.roseosporus a. Refractory Brick (SEM) b. Refractory brick c. Free mycelium d. Silk sachets e. Pellets (cross-section).

The photographs show the inner pores of carriers used, which were densely populated by the immobilized cells. The porous network was covered with the *S. roseosporus* cells which were adsorbed on to the matrix surface. The electron microscopic view of the immobilized cells revealed their dense and compressed structure. The mycelial network was compact and condensed to a smaller area. The silk sachets packaged the mycelium well enough but did not compress them much. The elongated, free mycelium were distributed over the space while the pelletized cells

4.7.6 Rheological characterization of the broth

Figure 4.30 shows that morphological changes and rheological properties of *S. roseosporus* were interdependent phenomena. The broth viscosity increased over the time for both free and pelletized cells. The specific cell growth rate was more for the free mode of cells as compared to immobilized cells. The free cells accumulated as dense aggregates and resulted in viscous broth during the course of fermentation. The viscosity increased three times almost the initial value. Thus, the oxygen mass transfer affected a lot. The pellets were comparatively stable but the dense growth of cells over the time led to 1.5 times increase in viscosity which in turn reduced oxygen transfer. The slow and steady growth of immobilized cells helped them to overcome the viscosity issue and hence improve the hydrodynamics of the system.

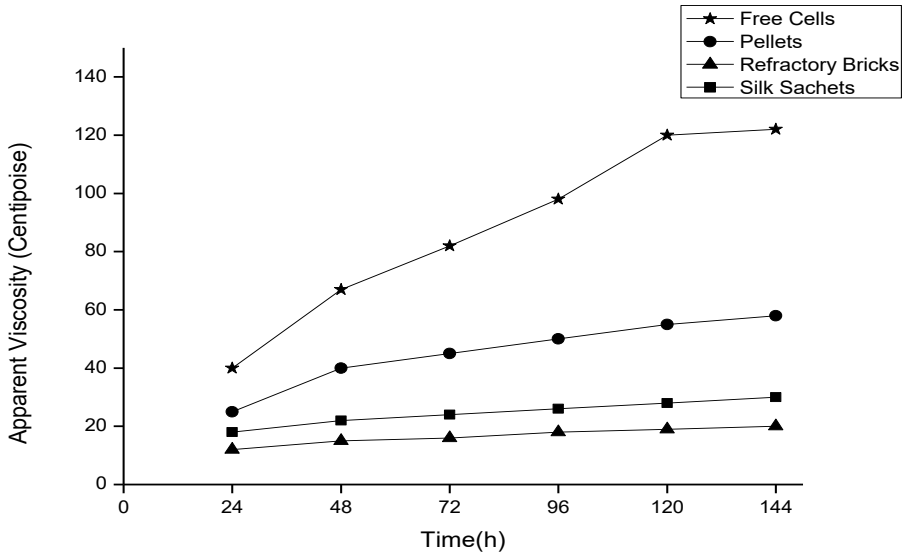

Fig. 4.30 Apparent viscosity of the fermentation broth over the time

4.7.7 Variation of volumetric oxygen transfer coefficient

The variation of volumetric oxygen transfer coefficients by immobilized cells on different adsorbent was compared with free cells. It was observed that, with free cells, the volumetric oxygen transfer coefficients could be maintained at 20 h^{-1} at 144 h as depicted in Figure 4.31. This effectively resulted in reduced Daptomycin production. However, with the use of immobilized modes, volumetric oxygen transfer coefficient (K_La) improved as fluid viscosity of the broth was much better controlled. Volumetric oxygen transfer coefficients were observed at 132 h as 85 $h^{-1}$and 80 h^{-1} respectively for refractory bricks and silk sachets. Low volumetric oxygen transfer coefficient (K_La) value was obtained for pellets as compared to other carriers due to the change in rheological properties of the fermentation broth. Broth viscosity and oxygen mass transfer were much controlled in case of immobilized cells.

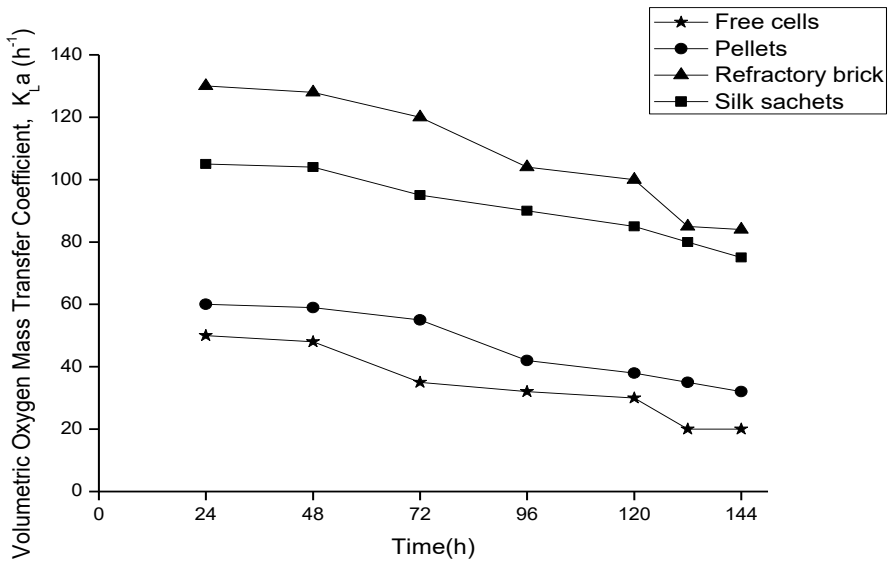

Fig 4.31 Volumetric oxygen mass transfer patterns over the time

4.7.8 Comparison of Daptomycin Production by free and immobilized cells of *S.roseosporus*.

The consolidated data in Table 4.8 shows that in a single batch, pelletized cells and free cells depicted considerable production ability. Pellet growth offered advantages over the free cells and the regulation of hyphal extension and pellet size are of great importance. But the reusability and controlled fluid viscosity of immobilized cells had an edge over them.

Table 4.8 Comparison of Daptomycin Production for different modes of cell immobilization

Carrier material	Daptomycin concentration(mg/l)(after first batch)	Daptomycin concentration(mg/l)(after final batch)	Reusability upto (cycles)
Free cells	750	750	NIL
Pellets	810	1430	2
Refractory brick	700	4895	8
Silk sachets	620	3623	6

This is beneficial for antibiotic fermentation which is non growth associated [Ramakrishna and Prakasham 1999]. The increased production of Daptomycin in immobilized system over free cells is accounted due to changes in permeability of cell walls well as reusability of the matrices [Morikawa et al. 1979]. For pelletized cells, the reusability was limited up to two cycles as the cells degenerated, showed dense aggregates and hence increased broth viscosity.

1430 mg/l of Daptomycin was produced using pellets for 2 batches. Immobilized cells on refractory bricks and silk sachets led to 4895 mg/l and 3623 mg/l Daptomycin production respectively. The cell leakage, increased viscosity and cell degeneration over the time led to lesser reusability of silk sachets than refractory bricks. The high oxygen demand of the Daptomycin production processes may be attributed to its demand in the biosynthetic pathway. The biosynthetic pathway of Daptomycin shows that there are two crucial

oxygen consuming steps in the pathway [Tally and De Bruin 2000; Robbel and Marahiel 2010]:

a. The initiation step of Daptomycin formation requires oxygen where lipidation by DptE and DptF takes place. Decanoic acid is activated by the putative adenylating enzyme DptE under ATP consumption. The fatty acid is then transferred onto acyl carrier protein DptF. The C domain of DptA is predicted to catalyze the condensation reaction between fatty acid and

N-terminal tryptophan.

b. The cyclization and elongation of the peptide chain where an adenylation domain selects the amino acid monomer to be incorporated and activates the carboxylate with ATP to make the aminoacyl-AMP.Next, the A domain installs an aminoacyl group on the thiolate of the adjacent T domain. The condensation (C) domain catalyzes the peptide bond forming reaction, which elicits chain elongation.

The dense network of the free cells led to three phase fluid viscosity which hampered the oxygen mass transfer into the cells. For the immobilized system, the three phase broth viscosity was much better controlled and the hydrodynamics improved over the time. Volumetric oxygen transfer coefficients observed at 132 h were 85 h^{-1} and 80 h^{-1} for refractory bricks and silk respectively whereas that for pellet and free cells was low. The present study confirmed that Daptomycin production with whole cell immobilization strategy in an airlift bioreactor showed improved results. Therefore, whole-cell immobilization can be considered as a useful strategy for enhanced production of this important life-saving drug. Further, efforts can be taken to improve the mass transfer characteristics of the free cell systems.

4.8 Effect of Bubble Characteristics on Mass Transfer Coefficient in an Internal Loop Airlift Bioreactor for Microbial Production of Daptomycin

4.8.1 Bubble Characterization

The bubble size distribution inside the airlift bioreactor is shown in Table 1. The results reveal that the sauter mean bubble diameter is smaller for the multiple hole sparger than that for the single hole sparger under the same superficial gas velocity.

Table 4.9 Bubble characteristics under different superficial gas velocities for different spargers.

Superficial gas velocity Usg(m/s)	**Single Hole Sparger**		**Multiple Hole Sparger**	
	Sauter Mean Bubble Diameter (m)	**Bubble Number (1/L)**	**Sauter Mean Bubble Diameter (m)**	**Bubble Number (1/L)**
0.001	0.0036	750	0.0025	2500
0.002	0.0038	1100	0.0028	3035
0.003	0.0039	1580	0.0030	3200
0.004	0.0042	1855	0.0036	4100
0.005	0.0044	2020	0.0038	4500

The bubble number significantly increases with increasing superficial gas velocity for both the spargers. The bubble number of the multiple hole sparger is quite larger than that of the single hole sparger under the same superficial gas velocity.

4.8.2 Gas holdup

The gas hold up values were calculated using bubble diameter and number of bubbles for each diameter as a function of superficial gas velocity as depicted in Figure 4.32.The value of gas holdup of the multiple holes sparger was higher than that in the single hole sparger. Small bubbles rose slowly and stayed longer in contact with the liquid media which allowed enough time for oxygen to dissolve and distribute. Small bubbles produced in large numbers led to higher gas holdup values. Due to higher number of bubbles generated in case of multiple hole sparger, the overall gas holdup increases almost linearly with the superficial gas velocity.

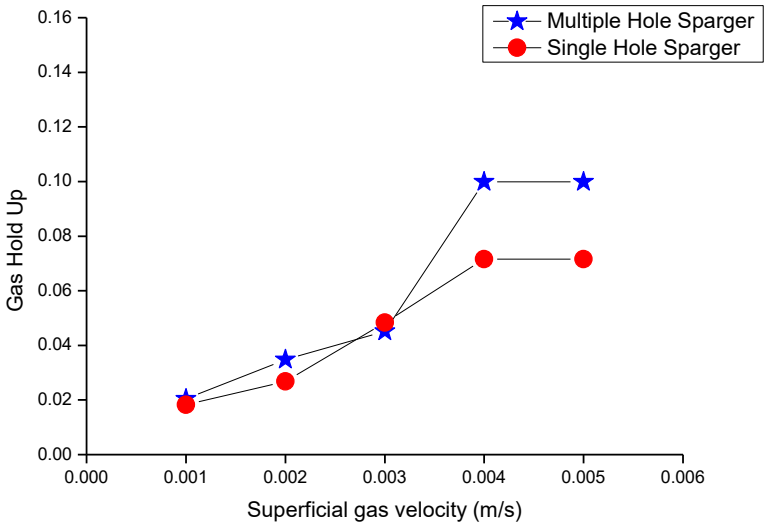

Figure 4.32 Evolutions of gas hold up with superficial gas velocities for different spargers

At higher superficial gas velocity, bubble swarms and the bubble coalescence make flow pattern complicated, resulting in slow rise of gas holdups. Similar results were obtained by Chisti [Chisti,1989] . As shown in Figure 4.32, the overall gas holdup obtained with

the multiple hole sparger is higher than that of single hole sparger. Therefore, the larger number of holes lead to larger number of bubble formation and of small diameter which attributes for an overall increase of gas holdup for the multiple hole sparger [Lu *et al.*, 1991]. Moreover, the smaller bubble size and larger bubble numbers imply larger circulation of bubbles, leading to a higher gas holdup. The following equation establishes the correlation between the gas holdup and the superficial gas velocity [Chisti,1989]:

$$\varepsilon=\alpha U_{sg}^{\beta} \qquad (3)$$

where α depends on liquid physical properties as well as the reactor geometry, and β is generally found to be a value ranged from 0.4 to 1 [Jin *et al*.,2006].Fitting Eq. (3) to the experimental data of different spargers, the parameters determined by the regression are listed in Table 4.10.

Table 4.10 Parameters of correlations between the gas hold up and the superficial gas velocity for different spargers.

Sparger type	**α**	**β**	**R^2**
Single Hole Sparger	0.0161	1.0274	0.987
Multiple Hole Sparger	0.0176	1.1478	0.996

The gas holdup estimated from bubble size and bubble number was quite consistent with the experimental data [Blažej *et al.,* 2004] obtained using bubble characteristics.

4.8.3 Mass transfer

The specific interfacial area and gas hold up can be related as:

$$a=\frac{6\varepsilon}{dB(1-\varepsilon)} \qquad (2)$$

Putting the experimental values in the equation (2), a higher gas holdup and a smaller mean bubble diameter lead to a larger specific interfacial area. Higher value of interfacial area is obtained for multiple hole sparger than single hole sparger at a given superficial gas velocity as shown in Fig. 4.33. The specific interfacial area increases linearly with increasing the superficial gas velocity. Since, K_La is directly proportional to the specific interfacial area, the increase of K_La arises mainly from the increase in the specific interfacial area. As the specific interfacial area can be expected to depend indirectly on the gas holdup [Abashar *etal.*,1998;Cerri *et al.*,2010; Wongsuchoto *et al.*,2003].

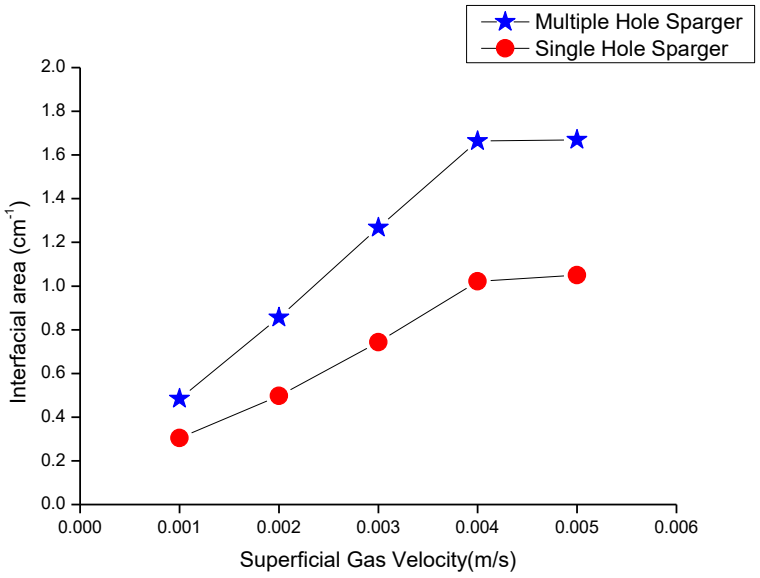

Figure 4.33 Interfacial areas with respect to different superficial gas velocities.

Experimental data of the volumetric oxygen transfer coefficient K_La for different spargers as obtained from dynamic gassing out method are plotted in Fig. 4.34. The data shows that the volumetric oxygen transfer coefficient increases almost linearly with the superficial gas velocity for both the spargers.

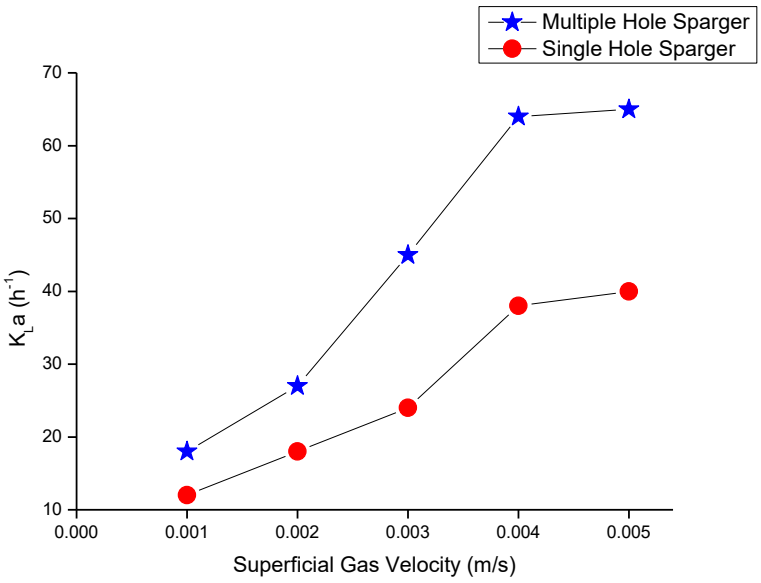

Figure 4.34 Evolutions of volumetric mass transfer coefficient with superficial gas velocity for different spargers.

It indicates that the K_La obtained with the multiple hole sparger is higher than that of single hole sparger. During fermentation, the K_La significantly increased from 30 $h^{-1}$for single hole sparger to 65 h^{-1} in case of multiple hole sparger [Cerri *et al.*,2010]. As applied for overall gas holdup, the following equation is applied to correlate the volumetric mass transfer coefficient with the superficial gas velocity:

$$K_La=\alpha U_{sg}^{\beta} \qquad (4)$$

The experimental parameters obtained for both spargers fitted well in the equation as shown in Table 4.11.

Table 4.11 Parameters of correlations between the volumetric oxygen transfer coefficient and the superficial gas velocity for different spargers.

Sparger type	**α**	**β**	**R^2**
Single Hole Sparger	0.2021	0.5792	0.9945
Multiple Hole Sparger	0.2843	0.7426	0.9839

The superficial gas velocity directly affects gas holdup. The gas holdup further affects the specific interfacial area and thus, volumetric oxygen transfer coefficient. However, the relationship between superficial gas velocity and volumetric oxygen transfer coefficient is also influenced by bioreactor geometry, sparger designs, three-phase mixing and flow patterns making it elaborate and complicated. The influences of the sparger designs on hydrodynamics and mass transfer characteristics in a sparged internal loop airlift bioreactor have been investigated for fermentation process. It is found that gas holdup and volumetric oxygen transfer coefficient is strongly related to the sparger design and especially the superficial gas velocity. The comparison between experimental data of the single hole sparger and the multiple hole sparger indicated that the sparger with the larger number of orifices was more efficient for the mass transfer, because it produced a smaller mean bubble diameter and larger number of bubbles leading to greater gas hold up values as compared to single hole sparger. Moreover, for a given sparger structure, the effect of the superficial gas velocity on the K_La was mainly reflected on the specific interfacial area as calculated using gas hold up values. Empirical correlations could predict the hydrodynamic parameters for the overall gas holdup and the volumetric oxygen transfer coefficient for different spargers. The empirical correlations had satisfactory agreement

with the experimental results obtained. Therefore, it could be concluded that the bubble characteristics could be utilized to study the hydrodynamics inside an airlift bioreactor and sparger geometry could be used to improve the oxygen mass transfer characteristics of the fermentation broth and hence to ameliorate the production of Daptomycin.

4.9 In-Vitro Assessment of the Synergistic Oligodynamic Potential of Daptomycin and Mycogenic Gold, Silver and Bimetallic Nanoparticles for Prevention of Skin Infections

4.9.1 Nanoparticle formation

The bioconversion of noble metal salts to metal nanoparticles is depicted in Figure 4.35 as noted by visual observations. It was noticed that the color varied for blank, gold chloride supplemented broth, silver nitrate supplemented broth and for the combination of both gold and silver salts. Fungal culture of *Aspergillus niger* MTCC 1025 started to show visual changes within 8 hours which intensified on further incubation. Culture reacted with 0.2mM $HAuCl_4$, 0.2mM AgNO3 and 0.2mM (HAuCl4:AgNO3). Silver salt supplementation showed Yellow colour, bimetallic salt supplementation revealed Reddish colour and Gold salt supplementation gave Lavender colour. After filtration of the particles, the media colour remained colourless whereas the cell mass retained the characteristic inferring it to be intracellular Nanoparticle formation. Therefore, further sonication and filtration was done [Shankar *et al.*, 2004].

Figure 4.35 Formation of silver nanoparticles, gold nanoparticles and bimetallic gold and silver nanoparticles

The nanoparticles produced were kept in the dark at 4^{o}C and even after one month, no major changes were observed (color or any physical appearance) making it stable [Shedbalkar *et al.*, 2014].

4.9.2 UV-Vis Spectroscopy

Fungal culture exposed to metal salts for 18-24 hours were tested for UV-Vis Spectroscopy. No characteristic peaks were obtained for the mold media taken as blank. Concluding it to be intracellular nanoparticles production. Further, sonicated samples of the culture incubated with metal salts were analyzed which gave specific peaks showing nanoparticle formation as shown in Figure 4.36.

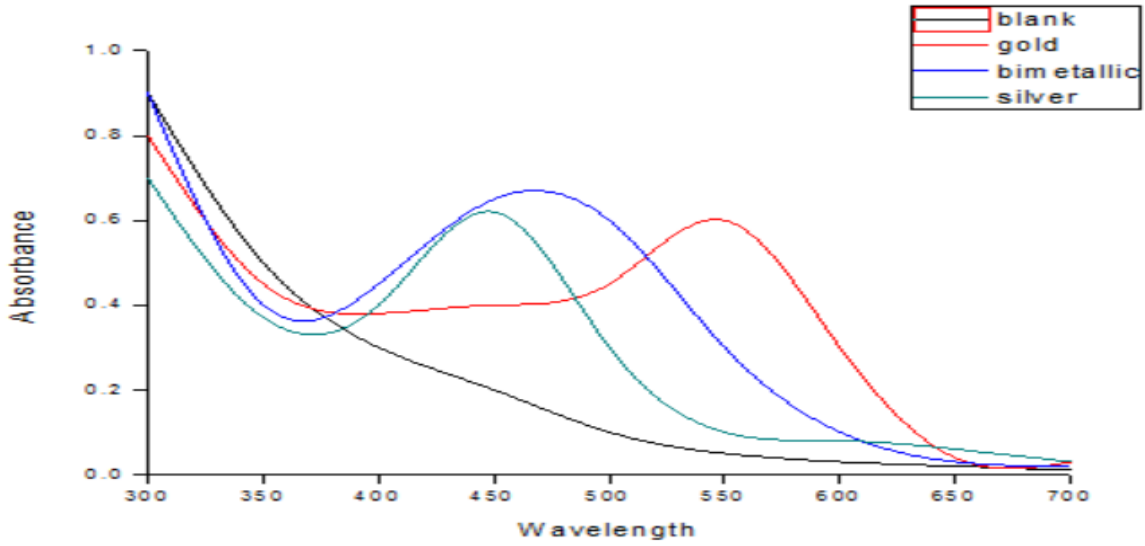

Figure 4.36 UV-Vis spectrum for Au, Ag and Au/Ag nanoparticles

The presence of Gold nanoparticles showed peak at 550nm,Silver nanoparticles indicated peak at 450nm and Bimetallic nanoparticles showed an intermediate peak at 480nm[Hurtado *et al.*, 2017].

4.9.3 X-Ray Diffraction

Further the evidence for the formation of Gold Silver Bimetallic Nanoparticles was provided by the X-Ray Diffraction analysis. The crystalline nature of bi-metallic nanoparticles synthesized by *Aspergillus niger* was determined by Bragg's diffraction peaks evident from XRD pattern as shown in Figure 4.37. All these values showed the Face Centred Cubic (FCC) structure of the obtained nanoparticles having different lattice planes. The Bragg's peak positions in the spectrum and their intensities were compared with standard JCPDS files [JCPDS file nos 04-0783 and 01-1174, respectively. The remaining unidentified peaks in XRD pattern including a sharp peaks can be attributed to the crystalline nature of capping and stabilizing proteins present over the surface of synthesized Gold, Silver and bimetallic nanoparticles from *A.niger* [Mukherjee *et*

al.,2008]. The mean diameter of the Au-Ag NPs was calculated from the XRD pattern according to the line width of the maximum intensity reflection peak using the Debye Scherrer's equation:

$$D = \frac{K\lambda}{\beta 1/2 \ \cos\theta}$$

Where K is a dimensionless shape factor with a value close to unity, λ is the X ray wavelength in angstrom, $\beta_{1/2}$ is the width of the XRD peak at half height and θ is the Bragg's angle. Thus, the XRD pattern clearly shows that the Au-Ag NPs were formed by the reduction of metal ions and are crystalline in nature.

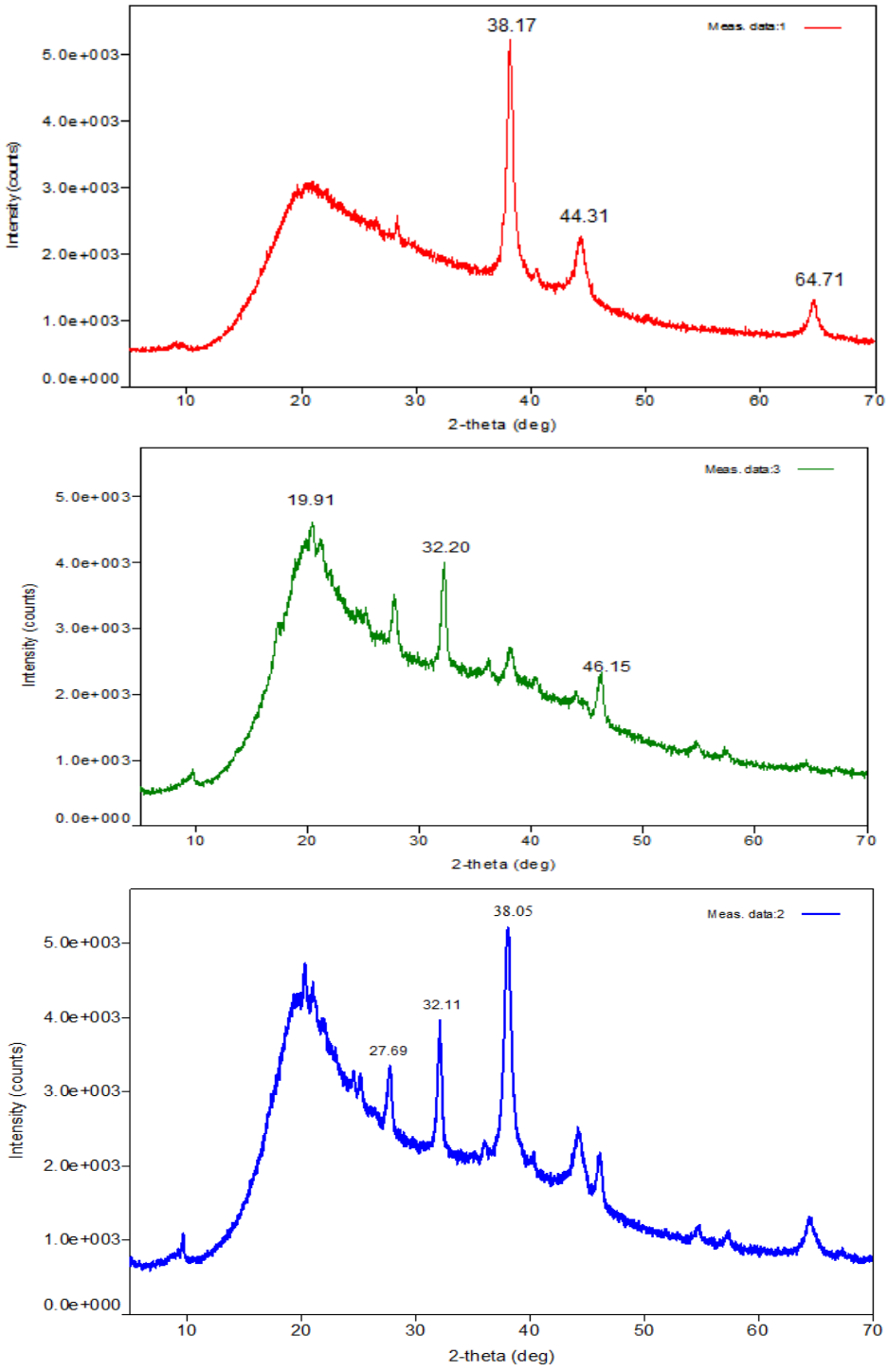

Figure 4.37 XRD profiles for A) Gold nanoparticle (Red) B) Silver nanoparticle (Green) C) Bimetallic nanoparticle (Blue)

The XRD image of the sample after treating it with gold chloride is depicted in Figure 4.37a. A strong signal can be seen at 38.17^{o} which represents presence of gold and the value is consistent. The three strong Bragg's diffraction peaks at 38.17^{o}, 44.31^{o}, 64.70^{o}

[Sawle *et al.*,2008]. So particle sizes were calculated to be 20.2 nm, 10.48 nm, 10.22nm . The XRD image of the sample after treating it with Silver Nitrate showed a strong peak at 19.91^{o} which represents presence of Silver and the value is consistent in Figure 4.37 b. It showed three strong Bragg's diffraction peaks at 19.91^{o}, 32.20^{o}, 46.15^{o}. Particle sizes evaluated were 4.97nm, 30.48nm and 19.65nm. A strong signal can be seen at 22.69^{o} which represents presence of Bimetallic and the value is consistent. The three strong Bragg's diffraction peaks at 22.69^{o}, 32.11^{o}, 38.05^{o}. Particle sizes identified as 19.27nm, 35.01nm and 39.71nm.The XRD patterns clearly showed that Nanoparticles were crystalline in nature [Basavaraja *et al.*, 2008; Shankar *et al.*, 2003].

4.9.4 Transmission Electron Microscopy (TEM) Analysis

Transmission electron microscopy study is shown in (Figure 4.38). The homogeneity in nanoparticles was evident in case of metallic nanoparticles produced. No particular core-shell arrangement was seen for the silver-gold bimetallic nanoparticles. The characterization results concluded monometallic gold and silver nanoparticles and alloy (mixtures of silver and gold nanoparticles in random configuration) sort of bimetallic nanoparticles. TEM images clarified that gold, silver, bimetallic nanoparticles formed were characterized by uniform distribution with spherical shape [Tamuly *et al.* ,2013].

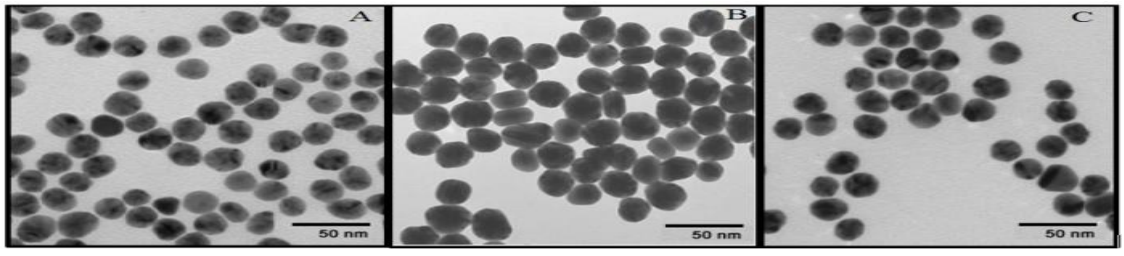

Figure 4.38 TEM images of A) Gold nanoparticle B)Silver nanoparticle C)Bimetallic nanoparticle

4.9.5 Antimicrobial assay

The antibacterial effect of individual nanoparticles, Daptomycin and Daptomycin in combination with nanoparticles was observed through disk diffusion method as shown in Figure 4.39. The process was non-toxic and eco-friendly. The combinatorial effect led to the higher binding affinity of the drug and enhanced antimicrobial efficacy [Fakhri *et al.*, 2017].

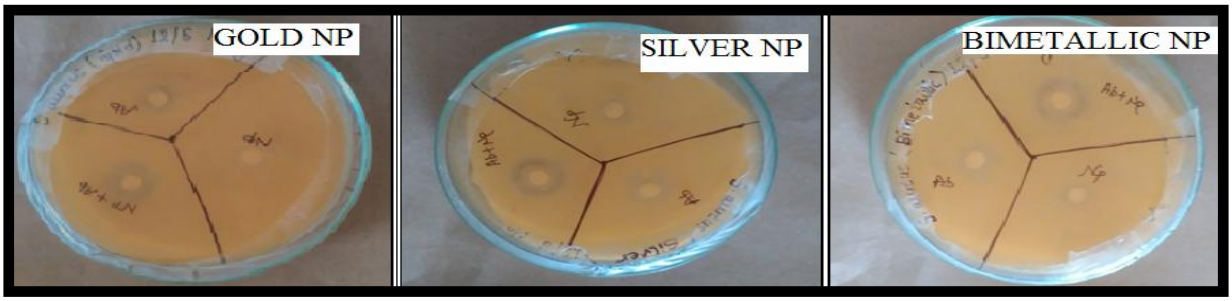

Figure 4.39 Antimicrobial assay against *S.aureus;* Antimicrobial assay against *S.aureus;*Zone of inhibition formed A)Gold nanoparticle B)Silver nanoparticle C)Bimetallic nanoparticle

Table 4.12 depicts the antimicrobial effect of Daptomycin along with nanoparticles in topical gel formulation to combat skin infections by *S.aureus*. The antibiotic combined with bimetallic nanoparticles showed improved bactericidal activity than free form of antibiotic. [Jadhav *etal.*,2016].

Table 4.12 Zone of inhibition (mm) for free Daptomycin and Daptomycin combined with bimetallic nanoparticles

Type of Noble Metal Nanoparticles	**Zone of Inhibition(mm)**			**Increased zone size (mm) (b-a)**	**Fold increase % [(b-a)/a)]x100**
	Free Form of Nanoparticles	**Free form of Daptomycin (a)**	**Combined form of Daptomycin and Nanoparticles (b)**		
Bimetallic nanoparticles	8.12 ± 0.4	10.00 ± 0.2	14.32 ± 0.20	4.32	43
Silver nanoparticles	7.65 ± 0.1	10.00 ± 0.1	13.75 ± 0.43	3.75	38
Gold nanoparticles	7.00 ± 0.28	10.00 ± 0.4	13.00 ± 0.12	3.00	30
Average synergistic antimicrobial effect (%)					37

Free form of nanoparticles and Daptomycin were much less than their combined form which gave a synergistic antimicrobial or oligodynamic effect. This was evident from the increased zone of inhibition of antibiotic combined with bimetallic nanoparticles. There was 37% increase in efficacy of Daptomycin due to the synergistic effect with bimetallic

nanoparticles. The synergistic form of the drug prompted that the toxicity of high drug dosage can be mitigated in an economical way [Baker et al., 2017].